STUDY ON SILVER CONTAINING HZSM-5 CATALYSTS FOR ETHANOL CONVERSION TO AROMATICS

SURATSAWADEE SUWANNARAN

A THESIS SUBMITTED IN PARTIAL FULFILLMENT
OF THE REQUIRMENTS FOR THE DEGREE OF
MASTER OF SCIENCE IN PETROCHEMICALS AND
HYDROCARBON CHEMISTRY
SCHOOL OF GRADUATE STUDIES
KING MONGKUT'S INSTITUTE OF TECHNOLOGY LADKRABANG
2006

ISBN 974-15-2694-6

หัวข้อวิทยานิพนธ์	การศึกษาตัวเร่งปฏิกิริยา HZSM-5 ที่มีเงินเป็นองค์ประกอบสำหรับการเปลี่ยนเอทานอลเป็นสารอะโรเมติกส์
นักศึกษา	นางสาวสุรัสวดี สุวรรณารัณย์
รหัสประจำตัว	44065708
ปริญญา	วิทยาศาสตรมหาบัณฑิต
สาขาวิชา	ปิโตรเคมีและเคมีของไฮโดรคาร์บอน
พ.ศ.	2549
อาจารย์ผู้ควบคุมวิทยานิพนธ์	ผศ.ดร.ตะวัน สุขน้อย

บทคัดย่อ

วิทยานิพนธ์นี้เป็นการศึกษาการผลิตสารอะโรเมติกส์จากเอทานอลโดยตัวเร่งปฏิกิริยา AgHZSM-5 ซึ่งตัวเร่งปฏิกิริยาเตรียมจากการแลกเปลี่ยนไอออนของซีโอไลต์ NH_4ZSM-5 ด้วยไอออนเงิน การเร่งปฏิกิริยาดำเนินการในถังปฏิกรณ์แบบเบดคงที่ภายใต้ความดันบรรยากาศที่อุณหภูมิ 425 องศาเซลเซียส โดยศึกษาถึงอิทธิพลที่มีผลต่อการเร่งปฏิกิริยา เช่น W/F (6.7-27 กรัมชั่วโมงต่อโมล) อัตราส่วนของซิลิกอนต่ออลูมิเนียม (11 และ 28) ปริมาณเงิน (0.7-4.8 เปอร์เซ็นต์โดยน้ำหนัก) และการนำตัวเร่งปฏิกิริยากลับมาใช้ใหม่ โดยทำการวิเคราะห์ผลิตภัณฑ์ที่เกิดขึ้นด้วยเทคนิคก๊าซโครมาโตกราฟีแบบออนไลน์

จากการทดลองพบว่า W/F และความเป็นกรดของตัวเร่งปฏิกิริยาชนิด HZSM-5 มีผลอย่างมากต่อการกระจายตัวของผลิตภัณฑ์ โดยเมื่อ W/F เพิ่มขึ้นเอทิลีนจะลดลงและผลิตภัณฑ์ที่มีน้ำหนักโมเลกุลสูงเช่น อะโรเมติกส์จะเพิ่มขึ้น ความเป็นกรดมีความจำเป็นต่อปฏิกิริยาโอลิโกเมอไรเซชันของเอทิลีนและการเกิดสารประกอบอะโรเมติกส์ นอกจากนี้พบว่าตัวเร่งปฏิกิริยา HZSM-5(11) ที่มีเงินเป็นองค์ประกอบช่วยเพิ่มปฏิกิริยาอะโรมาไทเซชันของไฮโดรคาร์บอนเบาไปเป็นสารประกอบอะโรเมติกส์ โดยตัวเร่งปฏิกิริยาที่ให้ผลิตภัณฑ์อะโรเมติกส์สูงสุดคือ 0.7%AgHZ11 อย่างไรก็ตามในกรณีที่ใช้ AgHZSM-5(28) เป็นตัวเร่งปฏิกิริยากลับพบว่าเอทิลีนเกิดปฏิกิริยาโอลิโกเมอไรเซชันได้น้อยเพราะว่าตำแหน่งกรดบรอนสเตดของตัวเร่งปฏิกิริยานี้ไม่สามารถคงอยู่ได้ในระหว่างปฏิกิริยา อาจเนื่องมาจากไอออนเงินใน AgHZSM-5(28) ไม่สามารถถูกรีดิวซ์ได้ในปฏิกิริยาหรือกรดบรอนสเตดของ AgHZSM-5(28) สามารถทำปฏิกิริยากับโลหะเงินกลับไปเป็นไฮโดรเจนและไอออนเงินได้ (Reversible interconversion)

Thesis Title	Study on silver containing HZSM-5 catalysts for ethanol conversion to aromatics.
Student	Miss Suratsawadee Suwannaran
Student ID.	44065708
Degree	Master of Science
Programme	Petrochemicals and Hydrocarbon chemistry
Year	2006
Thesis Advisor	Asst .Prof.Dr. Tawan Sooknoi

ABSTRACT

This thesis reviews the study on the production of aromatics from ethanol over AgHZSM-5. The catalysts were prepared by ion-exchange of NH_4ZSM-5 zeolite with silver cation. The catalytic testing was carried out in a fixed bed reactor at 425 ^{0}C under atmospheric pressure. The influence of reaction parameters, such as W/F (6.7-27g.h/mol), Si/Al ratio (11 and 28), silver content (0.7-4.8 wt.%) and regeneration of catalysts were investigated. The products were analyzed online by Gas Chromatography (GC).

The experiments show the strong influence of W/F and acidity in HZSM-5 on the product distribution. Ethylene is decreased and higher hydrocarbons such as aromatics are increased with increasing W/F. The acidity is essential for the ethylene oligomerization and aromatic selectivity. The incorporation of silver into HZSM-5 (11) zeolite appreciably enhances the aromatization activity of light hydrocarbons to aromatics. A high yield of aromatic hydrocarbons can be obtained with the 0.7%AgHZ11 zeolite. However, AgHZSM-5(28) is inactive for ethylene oligomerization, because the Brønsted acid sites cannot be retained during the reaction. This is probably because silver cation species in AgHZSM-5(28) may not be reduced during the reaction or the Brønsted acid sites in HZSM-5(28) may well react with reduced silver metal species forming hydrogen and silver cation (reversible interconversion).

ACKNOWLEDGEMENTS

The author wishes to express her sincere thanks to her advisor, Asst. Prof. Dr. Tawan Sooknoi for his supervisions, helpful suggestion and encouragement throughout this research. She is also grateful to Asst. Prof. Dr. Vanchat Chuenchom, Asst. Prof. Dr. Punnama Siriphannon and Asst. Prof. Dr. Piboon Pantu for serving as the chairperson and the committee, and valuable comment.

She would like to extend her sincere appreciation to all of her teachers, her friend and her research group for their constant guidance advice, support and encouragement.

The special thanks to Department of Chemistry, Kasetsart University for help in study on reduction of silver in zeolites. Thanks are also due to everyone who has contributed suggestion and supports throughout this work.

Sincere thanks to Mr. Artit Ausavasukhi for his advice, suggestion and kindness.

Sincere thanks to the department of Chemistry, Faculty of Science, King Mongkut's Institute of Technology Ladkrabang for equipment, chemicals and facilitates.

Finally, her deepest gratitude goes to her parents for their sincere love and concern, and for the hardship their encountered in these past twenty-seven years raising her and teaching her how to take care of herself and realized what life is and what it is for.

Suratsawadee Suwannaran

CONTENTS

Page

CONTENTS (continued)

Page

CONTENTS (continued)

LIST OF TABLES

Table Page

LIST OF FIGURES

Figure

CHAPTER 1

INTRODUCTION

1.1 Statement and significance of the problem

Many items in our everyday lives rely on products made by aromatics industry. They help to meet fundamental human need such as medicines, dyes and plastics, directly as a solvent and component of petrol. In today's chemical industries, aromatics largely produced from petroleum which is obtained from limited reserves. These finite reservoirs are highly concentrated in certain regions of the world. Therefore, those countries which not having these resources are facing a foreign exchange crisis, mainly due to the import of crude oil. Hence, it is necessary to look for alternative sources which can be produced from materials available within the country. As Thailand is an agricultural country, it is better if all the requirements of chemical industry and portions of other needs can be shared by agricultural products. Conversion of ethanol to aromatic hydrocarbons has received attention due to the raw material hold good promise. Ethanol can be obtained from fermentation of biomass, a renewable agricultural resource. Moreover, it can increase the value of agricultural products and reducing imbalance of trade problem.

This study was concerned with catalyst design for the conversion of ethanol with regards to high aromatic yields. HZSM-5 zeolites are known to convert methanol [1-2] and ethanol [3-4] into various hydrocarbons. However, the effort to enhance aromatic selectivity has focused on improving the dehydrogenation activity of this catalyst since HZSM-5 is a poor dehydrogenation catalyst. Recently, silver containing HZSM-5 can be served as a highly active dehydrogenation catalyst and shows a high selectivity for aromatics in conversion of methanol [5]. The Ag^+ ions in the zeolites are active centers for dehydrogenation of the intermediate alkenes. In conversion of ethanol, the major challenge is to develop the appropriate reaction condition over AgHZSM-5 for high aromatic yields. However, a detailed path way for this reaction have not been well established so far, as an attempt to obtain insight in this direction. Moreover, the study on influence of silver species over HZSM-5 on this reaction is interesting and such knowledge is quite relevant to the development of better catalysts.

1.2 Goal and objectives

The specific objectives of the study are as follows:

1.2.1 To obtain the appropriate reaction conditions for the conversion of ethanol over zeolite catalyst which allows high aromatic yields.

1.2.2 To understand the effect of silver species and its content in zeolite on aromatic yield.

1.2.3 To understand the behaviour of silver in AgHZSM5 for the ethanol conversion.

1.3 Scope of the study

1.3.1 Modification of NH_4ZSM5 zeolite with silver.

1.3.2 Characterization of the silver-modified zeolites by XRD, XRF, SEM, NMR and Gas adsorption analysis.

1.3.3 Investigation of appropriate W/F (W/F= 6.7-27g.mol/h).

1.3.4 Investigation of the effect of acidity in zeolite (Si/Al ratio=11 and 28).

1.3.5 Investigation of the effect of silver content in zeolite on aromatic yields(0.7-4.8 wt% silver loading).

1.3.6 Investigation of the effect of acidity on reduction of silver in zeolites by Temperature Program Reduction (TPR).

1.3.7 Analysis of the amounts of products from the reaction by GC.

1.4 Expected results

1.4.1 This research would provide the appropriate conditions and catalyst for producing high aromatic yields for ethanol conversion.

1.4.2 This research would provide not only a potential to develop a technology for producing aromatics from ethanol, but also a guide for converting agricultural product to high value products.

1.4.3 This research would provide the cleaner technology and appropriated policies on conservation of finite petroleum resources and investigation of alternative and renewable sources.

CHAPTER 2

THEORY AND LITERATURE REVIEWS

2.1 Ethanol

2.1.1 Ethanol production [6-7]

Ethanol is currently produced primarily through the fermentation of sugars. Many sorts of raw materials used in the ethanol production are conveniently classified under three types of agricultural raw materials; sugar, starches, and cellulose materials. The process uses enzymes to convert starches to simple sugars, and yeasts to ferment the sugars into ethanol.

Usually the fermentations proceed until the ethanol concentration reaches about 10%, when the activity of the yeast becomes inhibited by the alcohol. Finally, the fermented liquor is distilled, producing a constant-boiling (azeotropic) mixture of hydrous ethanol at 95.5% v/v. To produce anhydrous ethanol, the water is removed with dehydrated carbohydrate or, more recently, with an appropriately sized molecular sieve to which the water is adsorbed.

2.1.2 Ethanol fuels

Alcohols have been suggested as an engine fuel almost since automobile was invented [8]. However, some shortcomings of alcohols such as difficulties in their production and some unsuitable properties for engines have limited their widespread usage [8,9]. In recent years, the possibility of depletion of the world's crude oil reserves, increases in wholesale price of crude oil and increasing air pollution have increased the interest in alcohols [8–10].

Following effects on engine can be expected when ethanol is used as an engine fuel. Ethanol contains an oxygen atom therefore, it can be considered as a partially oxidized fuel [8]. For this reason, it has lower calorific value and stoichiometric air–fuel ratio than gasoline. Consequently, much more fuel is needed to obtain same performance when ethanol or ethanol–gasoline blends are used [11]. Ethanol has higher octane number than gasoline thus it can lead to operation at higher compression ratios therefore improvement in power output, efficiency and fuel consumption.

Furthermore, it has high latent heat of vaporization. As a consequence of both low calorific value and high latent heat of vaporization, engine volumetric efficiency may increase. However, vaporization of the intake mixture may be reduced. This problem can be avoided by heating intake manifold. It was reported that although vapor pressure of pure ethanol is low, Reid vapor pressure (RVP) of gasoline–ethanol blends rises depending on the ethanol proportion in the blend. Low RVP can cause cold starting problems, therefore, volatile additives should be used when pure ethanol is used. Furthermore, vapor lock may occur in the warm weathers. Because of the cooling effect on the intake charge and leaner operation, significant reductions in CO and NO_x emissions may be expected [8,11]. As known, ethanol has high affinity for water thus it contains certain amount of water. This is not a problem for pure ethanol because it is fully miscible with water but some serious problems can arise when gasoline–ethanol blends are used. Phase separation can occur in gasoline–ethanol blends since gasoline and ethanol are immiscible. This problem can be prevented by using semi-polar cosolvents (solubility improvers) such as isopropanol. On the other hand, water contamination of ethanol can cause corrosion on mechanical components [8]. Another important problem relating to use of ethanol in engines is that the emissions of formaldehyde, acetaldehyde and acetone are significantly increased [8,11].

Therefore, the conversion of ethanol to fuel over zeolite catalyst is an alternative way which not only corrects the ethanol as fuel problem, but also provides the benefits of ethanol produced by agricultural products. Moreover, catalytic conversion of ethanol produces single ring aromatics which are important petrochemical intermediates as well as valuable gasoline component. In the view of aromatic production, separation of BTEX aromatics from crude oil distillate is not feasible because they are present in low concentrations. Enriching naphtha fraction with these aromatics is possible mainly through a catalytic reforming process. However, raw materials in reforming process are produced from petroleum which are obtained from limited reserves.

2.2 Chemical reaction of ethanol to aromatics

The various yield of paraffinic, olefinic and aromatic hydrocarbons is indicative of a very complex series of reaction in the conversion of ethanol over HZSM-5.

The first step in this process is ethanol dehydration to produce ethylene which is the key intermediate for the reaction and the general pathway for production of different hydrocarbons has been proposed as follows:

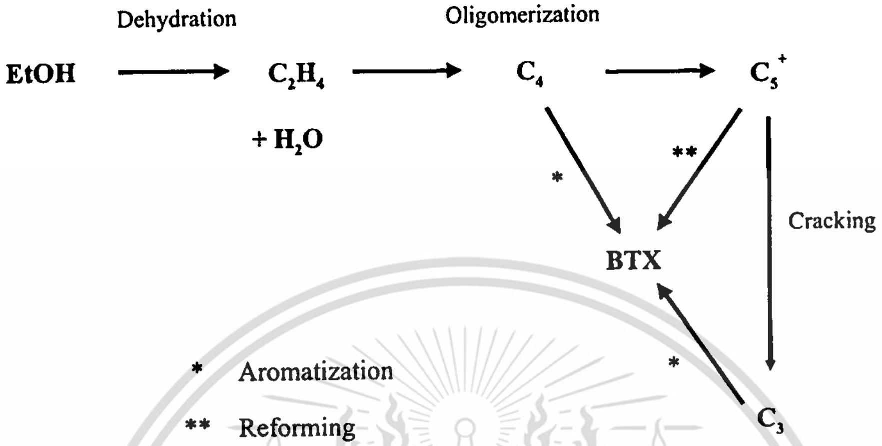

Once the first alkene is formed, it undergoes oligomerisations to form a near-equilibrium mixture of higher olefins. Finally, these higher alkenes cyclise to cycloalkenes, which in turn participate in dehydrogenation and hydrogen transfer with olefins to give aromatics [12]. Consecutively, hydrocarbons formed undergo a variety of acid catalyzed reactions, including double bond isomerisation, skeletal isomerisation, disproportionation and cracking. As a result of shape selectivity, ZSM-5 does not generate appreciable amounts of aromatics higher than C_{10}. Since they are consider to be coke precursors, the lack of higher aromatic compounds ensures sustained catalytic activity.

2.3 Zeolite[13]

Zeolites are microporous crystalline aluminosilicates, composed of TO_4 tetrahedra (T = Si, Al) with O atoms connecting neighboring tetrahedra. For completely siliceous structure, combination of TO_4 (T=Si) units in this fashion leads to silica framework, the +3 charge on the Al makes the framework negatively charged, and requires the presence of extraframework cations(inorganic and organic cations can satisfy this requirement) within the structure to keep the overall framework neutral. The zeolite composition can be best described as having three components:

$M_{n/m}^{m+}$	•	$[Si_{(1-n)}Al_nO_2]$	•	nH_2O
Extraframework cations		framework		sorded bed

The extraframework cations are ion exchangeable and give rise to rich ion-exchange chemistry of these materials. Cation concentration, sitting and exchange selectivity vary significantly with Si/Al ratios and play an important role in adsorption, catalysis and ion-exchange applications. Though acid site concentration decreases with increase in Si/Al ratio, the acid strength and proton activity coefficients increase with decreasing aluminium content. The novelty of zeolites stems from their microporosity and is a result of the topology of the framework.

2.3.1 ZSM-5 zeolite[14-16]

Zeolite ZSM-5 is a member of a new class of shape-selectivity catalysts with unique channel structures with differ from the familiar large pore faujasite and small pore zeolites such as erionite and Linde type A. They also possess unusual catalytic properties and have high thermal stability. The TO_4 tetrahedra can be combined in many arrays with sharing of O atom. When they are arranged as shown in Fig 2.1a, the result is the secondary building block of ZSM-5 and then are linked to form the chain-type building block shown in Fig 2.1b. The chain can be connected to form a layer as shown in Fig 2.2. Ring consisting of five O atoms are evident in this structure; the name of *pentasil* is therefore used to describe it. Also evident in Fig 2.2 are rings consisting of 10 oxygen atoms; these are important because they provide opening in the structure large enough for passage of even rather large molecule. The layer can be linked in two ways, the neighboring layer being related either by the operation of a mirror or an inversion. The former pertains to the zeolite ZSM-11, the latter to silicalite and ZSM-5; intermediate structures constitute the pentasil series.

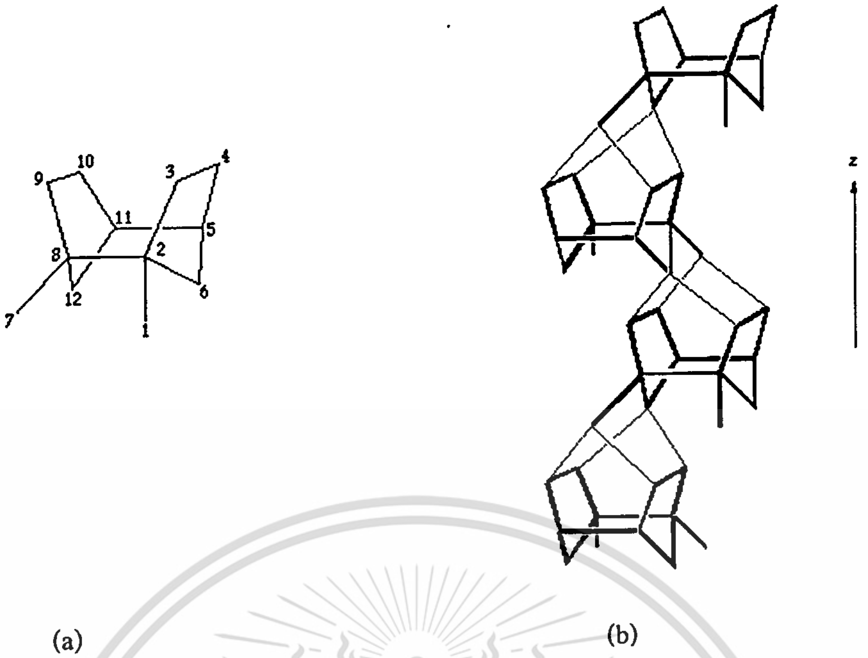

Fig2.1 (a) The secondary building block of ZSM-5, formed from TO4 tetrahedra. (b) The chain-type building block formed from secondary building blocks.

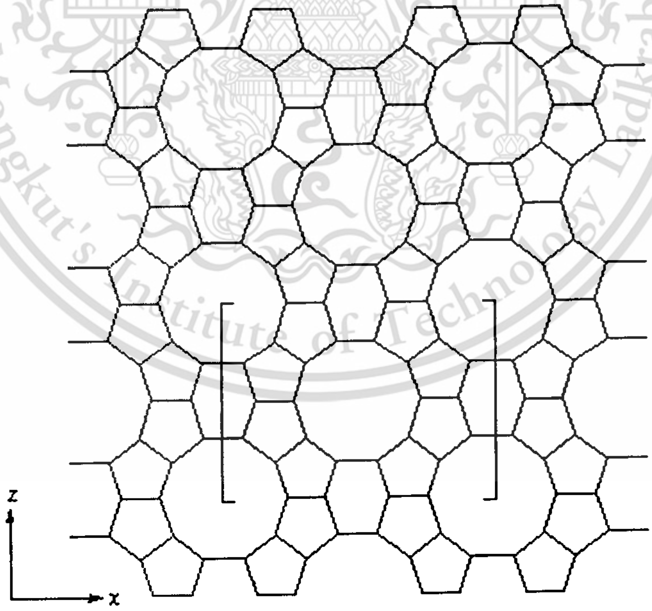

Fig2.2 Schematic diagram of ZSM-5 layer, formed by linking of the chains shown in Fig 2.1(b)

The three dimensional structure of ZSM-5 is represented in Fig 2.3a. The 10-membered rings provide access to a network of intersecting pores within the crystal. The pore structure is depicted schematically in Fig 2.3b; there is a set of straight, parallel pores intersected by a set of perpendicular zigzag pores.

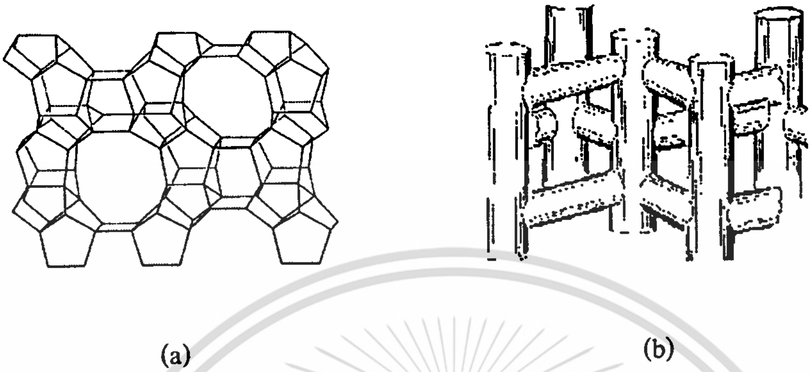

Fig 2.3 (a) Skeletal diagram of the (100) face of ZSM-5. (b) Channel structure of ZSM-5.

The unique catalytic properties of zeolite ZSM-5 are attributed to both the three-dimensional system of intersecting channels and its strong acid sites. ZSM-5 zeolite has pore system which believe to be significant for their unusually low coke formation. These factor make it sterically difficult for the formation of large polynuclear hydrocarbon responsible for coking and irreversible deactivation. This feature is probably one of the major reasons for the successful industrial application of these zeolites.

While most industrial application of zeolite catalysts make use of these in acid form. In ethanol conversion to aromatics, although HZSM-5 possesses excellent dehydration and oligomerisation properties, it is a poor dehydrogenation catalyst for aromatics selectivity and hence the catalyst requires modification by the addition of various promoters.

2.3.2 Metal-Doped Zeolites [17]

Zeolites are especially suitable as support materials for active components such as metal. Zeolite containing metal species is a bifunctional catalyst which possesses of both acid sites and metal centers. Suitable metals are effective catalysts for hydrogenations and oxidations, where by the shape selectivity of the carrier is retained. Important factors influencing the reactions of such bifunctional catalysts are the location of the metal, the particle size, and the metal-support interaction. The bifunctionality of metal-doped zeolite catalysis is explained here for the important example of isomerisation and hydrogenation. The metal content facilitates the hydrogenation and dehydrogenation step, while the acid-catalysed isomerisation step takes place under the restricted conditions of the zeolite cativties as shown in Scheme 2.1.

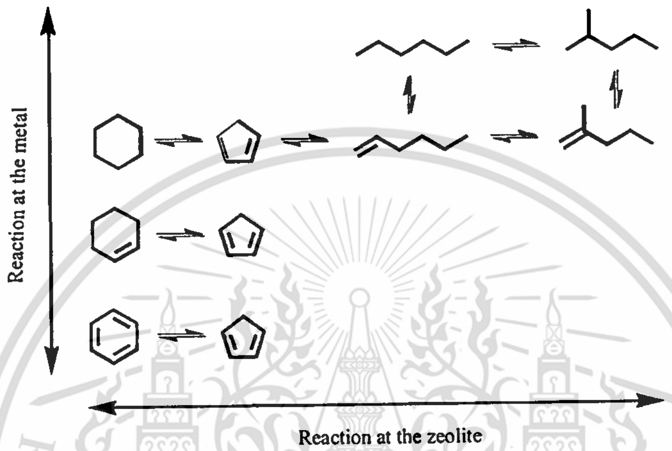

Figure 2.4 Bifunctionality of metal-doped zeolites: isomerisation and hydrogenation

The word " metal species" is used in the non-restrictive sense to describe species in their, not yet fully understood, valency. The advantage of bifunctional catalysis over the monofunctional acid catalysis is that the metal dehydrogenates the alkanes into alkenes which can further undergo a variety of acid catalyzed reactions to form desirable products.

2.4 Literature reviews

ZSM-5 type zeolite has been proved to be an efficient catalyst for the conversion of methanol and ethanol to various hydrocarbons [1-5]. Although more extensive works have been carried out on methanol conversion reactions on ZSM-5, works on ethanol conversion are rather limited. The conversion of ethanol to aliphatics and aromatics on HZSM-5 has been studied in a broad temperature range and with different acidity. The product distribution have been found to be strongly dependent on the temperature and the acidity of the samples [18]. For any particular zeolite, the amount of aromatics (benzene, toluene, xylene and mesitylene) in the product initially increases with rise in temperature and then decreases sharply. The conversion activity as well as the total aromatic products decrease with the decrease of strong acid sites and no aromatics are found at all below a limiting value of acid sites.

The effort to enhance aromatic selectivity have focused on improving the dehydrogenation activity of this catalyst since HZSM-5 is a poor dehydrogenation catalyst. According to the accepted mechanism, the initial products are lower alkenes. Aromatic hydrocarbons being formed via hydride transfer between the precursors such as alkenes and carbenium ions. This limits the yield of aromatics, since some formation of aromatics is inevitably accompanies by the formation of some alkanes. Therefore, if aromatics were produced through a direct dehydrogenation of alkene intermediates, the formation of alkanes could be suppressed and the selectivity for aromatics could be increased. ZSM-5 zeolites containing Zn or Ga ions are known to be effective in converting light alkane and alkene to aromatics [19-23]. These cations are also effective in dehydrogenation alkanes into aromatics. The light alkane aromatisation activity of the catalysts is in the order of ZnHZ ~ GaHZSM-5 > HZSM-5 [21]. However, the vaporisation of zinc from the Zn-doped catalyst was observed during reaction [22]. Since, in a reducing atmosphere, the zinc is maintained in a metallic state (not a metal oxide) and the metal zinc is vaporised at about 400^0C. It is unavoidable for it to melt and have evaporation loss from the catalyst, resulting in a remarkable reduction in aromatic selectivity. The effect of metal cations other than Zn and Ga cations have scarcely been explored. Recently, Ag-ZSM-5 has also been found to be very effective for aromatisation of alkanes, alkenes and methanol [5,24]. Loading of Ag^+ ions greatly enhances the C-H bond cleavage of the starting alkanes. Over HZSM-5, the C-C bond cleavage is predominant as compared to the C-H bond cleavage [5]. The rate of hydrogen formation over AgHZSM-5 is 15 times higher than over H-ZSM-5, while the formation of methane and ethane was rather depressed by introducing Ag^+ ions into HZSM-5. On the other hand, both C-H and C-C bond cleavage are enhanced over Ga and Zn-ZSM-5. Therefore, it is expected that the use of Ag-ZSM-5 as a catalyst in the ethanol conversion would increase the selectivity forwards aromatics. Moreover, modification of zeolites with silver by different ways has led to other applications, such as selectively catalytic reduction (SCR) of NO_x by hydrocarbon. It is believed that Ag^+ ion is active species for SCR of NO_X over Ag loaded catalysts

[25-27]. On the other hand ,it is recently reported that the formation of cationic $Ag_n^{\delta\cdot}$ cluster ($2 \leq n \leq 4$) species is highly active for NO_x reduction, independently on zeolite types [28].

CHAPTER 3

EXPERIMENTAL DETAILS

3.1 Reagents

Chemicals	Grade of purity	Manufactures
3.1.1 Air	Air Zero	TIG
3.1.2 Acetone	99.5%	CARLO ERBA REAGENTI
3.1.3 Benzene	99.8%	CARLO ERBA REAGENTI
3.1.4 Cumene	≥98%	Fluka chemical
3.1.5 Cyclohexane	≥98%	CARLO ERBA REAGENTI
3.1.6 Distilled water	-	-
3.1.7 Ethyl alcohol absolute	99.8%	CARLO ERBA REAGENTI
3.1.8 Ethylbenzene	≥98%	Fluka chemical
3.1.9 Ethylene gas	≥99.5%	TIG
3.1.10 Helium gas	High purity	TIG
3.1.11 *n*-Heptane	99%	CARLO ERBA REAGENTI
3.1.12 *n*-Hexane	99.9%	Mallinckrodt
3.1.13 Hydrochloric acid	37%	MERCK
3.1.14 Hydrofluoric acid	48%	MERCK
3.1.15 Hydrogen gas	High purity	TIG
3.1.16 LPG	-	SIAM GAS
3.1.17 Molecular sieve 13 X	-	Fluka chemical
3.1.18 Nitrogen gas	High purity	TIG
3.1.19 *n*-Nonane	>99%	MERCK
3.1.20 Silver nitrate	>98.5%	CARLO ERBA REAGENTI
3.1.21 Toluene	99.8%	MERCK

Chemicals	Grade of purity	Manufactures
3.1.22 Xylene	>98.5%	Fluka chemical
3.1.23 Zeolite NH_4ZSM-5	-	Zeolyst

3.2 Apparatus

3.2.1 Buchner flask

3.2.2 Buchner funnel

3.2.3 Catalytic testing rig

3.2.4 Clamp

3.2.5 Gas adsorption analyzer (Autosorb-1C, Quantrachrome)

3.2.6 Gas chromatography (Buck scientific, model 910)

3.2.7 Heating mantle

3.2.8 Heating Tape

3.2.9 Laboratory glassware

3.2.10 Magnetic stirrer

3.2.11 Nuclear Magnetic Resonance Spectrometer (AVANCE DPX300, Bruker)

3.2.12 Oven

3.2.13 Peristaltic pump (WATSONMARLOW, 101U/R)

3.2.14 Sieve (U.S.A standard sieve, AASHO N-92)

3.2.15 Scanning Electron Microscope (LEO 1455VP, LEO Electron Microscopy, Scientific Service Centre, KMITL)

3.2.16 Vial

3.2.17 Wash bottle

3.2.18 Water circulator

3.2.19 X-ray Fluorescence Spectrometer (SRS 3400, Bruker AG, Scientific Instrument Service Centre, KMITL)

3.2.20 X-ray Powder Diffractometer (D8 Advance, Bruker AG, Scientific Instrument Service Centre, KMITL)

3.3 Process of study

A process of the study of the ethanol conversion to aromatics over zeolite catalyst comprises the following stages:

3.3.1 Modification of zeolites

NH_4ZSM-5 (Si/Al ratios of 11 and 28) were obtained from Zeolyst. HZSM-5 was prepared from NH_4ZSM-5 by calcining at 550°C for 4 hours in dry air.

Silver incorporated HZSM-5 catalysts were prepared by an ion-exchange method using NH_4ZSM-5 zeolite as a starting material. Ion exchange of silver was carried out at room temperature with various concentrations of aqueous silver nitrate solution as shown in Table 3.1. Since silver materials are sensitive to light, all above procedures are carried out in the dark. After the exchange, the sample was washed by water circulator. After filtration, the zeolite was dried at 120°C for 3 hours and activated in air at 550°C for 4 hours. This catalyst is referred to as AgHZSM-5. In the case of reduction, this catalyst was further activated under stream of hydrogen at 425°C for 2 hours. This catalyst is referred to as red-AgHZSM-5. The catalyst with different silver content will be designated as (%wt of Ag) AgHZ (Si/Al ratio), e.g. 0.7%AgHZ11 and 3%red-AgHZ28.

Table 3.1 List of the Ag ion-exchanged zeolites used in the study

Catalyst	$AgNO_3$ Concentrations(M)	Time(hr)	Repeat
0.7%AgHZ11	5×10^{-4}	0.5	1
1.3%AgHZ11	1×10^{-3}	0.5	1
3.0%AgHZ11	1×10^{-3}	24	2
4.8%AgHZ11	5×10^{-3}	1.5	1
3.0%AgHZ28	1×10^{-2}	13.5	1

3.3.2 Characterization of catalysts

3.3.2.1 Crystal morphology of zeolites

Scanning electron microscopy (SEM) is the most versatile technique to study the morphology and crystal size of zeolites. The sample was finely divided onto a sample holder. The sample surface was then coated with gold thin film. After that the sample holder was left in the sample chamber, and evacuated from ambient pressure to 10^{-4} torr or less. The holding sample can be adjusted and moved in the X,Y and Z directions. As a consequence, the sample can be viewed from almost any perspectives.

3.3.2.2 Zeolites structure

The zeolite structure was checked by X-ray diffraction (XRD). The sample was finely grinded to a permit packing of the sample into an XRD sample holder. The XRD pattern was obtained by scanning over the angle range from $2\Theta = 5$ to 60° with a step angle of 0.04 degree per step and detection time 1.0 seconds. The X-ray source is $Cu\text{-}K\alpha$ generated at a voltage of 40 kV, 40 mA.

3.3.2.3 Chemical composition of the zeolite samples

The chemical composition of the catalysts was determined by X-ray fluorescence spectroscopy (XRF). The sample was prepared by mixing 4.5 g of boric acid and 0.5 g of zeolite and sent to grinder. The mixture was packed onto sample holder and compressed at 150 KN. The sample will then be placed in the sample chamber of X-ray fluorescence spectroscopy. Rhodium is used as source for analysis at 50 KV, 60 mA.

3.3.2.4 Surface area

Gas adsorption analysis is the technique used for surface area determination of the porous materials. The zeolite sample was weighed about 20 mg and transferred to a clean, dry empty sample cell. This sample cell was loaded to the outgassing station. Then heating mantle was installed with the sample cell and temperature was raised to 350°C under vacuum. The sample was out-gassed about 18 hours. The sample cell was then removed from the out gassing station after the nitrogen was filled and loaded to the analysis station. The equilibration time was set to 3 minutes and the nitrogen adsorption was measured at the partial pressure (P/P_0) ranged from 10^{-6} to 1.0 at $-195.6^{\circ}C$. When adsorption was complete, the sample cell was removed from the sample station and then dried thoroughly and reweighed.

3.3.2.5 Acid site

Acid sites of zeolite were investigated by nuclear magnetic resonance (NMR). The measurement was performed on a Bruker ADVANCE DPX300 NMR spectrometer at 300-MHz with BBI MAS probe. Prior the measurements, catalyst was packed in 5 mm ZrO_2 rotor and heated up to 270 and 360 °C with high vacuum ($3.0x10^{-5}$ torr). After the sample was cooled to room temperature, it was filled in helium and transferred to the spectrometer. Sample was spun at 5 kHz, a spin echo pulse was used to acquire ^{1}H spectra with 64 scans for each spectrum and chemical shifts were referenced to adamentane.

3.3.2.6 Reduction of silver in zeolite

The reduction of silver in zeolite was characterized by Temperature program reduction (TPR). Prior to the TPR experiment, catalyst was pretreated in a flow of Ar at $550^{\circ}C$ for 1 hour, and then was cooled to $80^{\circ}C$. H_2-TPR was carried out from $50^{\circ}C$ to $800^{\circ}C$ using $2\%H_2/Ar$ as a reducing gas (30 ml/min) at heating rate of $10^{\circ}C/min$ and the change in the H_2 concentration was monitored with thermal conductivity detector (TCD).

In the case of temperature-programmed hydrogen evolution (TPHE). Catalyst sample was reduced in a flow of 2% H_2/Ar at $425^{\circ}C$ for 2 hours, and then cooled to $80^{\circ}C$ in a flow of Ar. TPHE was carried out from $80^{\circ}C$ to $800^{\circ}C$ in a flow of Ar and the evolved H_2 was measured using mass spectrometer as the detector.

3.3.3 Catalytic testing

The catalytic activity was carried out at atmospheric pressure in a fixed bed flow reactor. The reactor was made with a borosilicate glass tube (6 mm i.d). The catalyst (180-250μm) was packed in the middle of the reactor. W/F of 6.75-27 g.h/mol were investigated. Before reaction, the catalysts was pretreated under air stream at $550^{\circ}C$ for 1 hour and then cooled to $425^{\circ}C$ in a flow of nitrogen.

Liquid ethanol was pumped from a graduated cylinder using a peristaltic pump at a flow of 0.01 mol/hour. The vaporize ethanol feed was then carried by the nitrogen gas (32 ml/min) and pass to the reactor. The schematic diagram of the experimental setup is shown in Figure. 3.1. In order to prevent condensation of products, the line after reactor was heated.

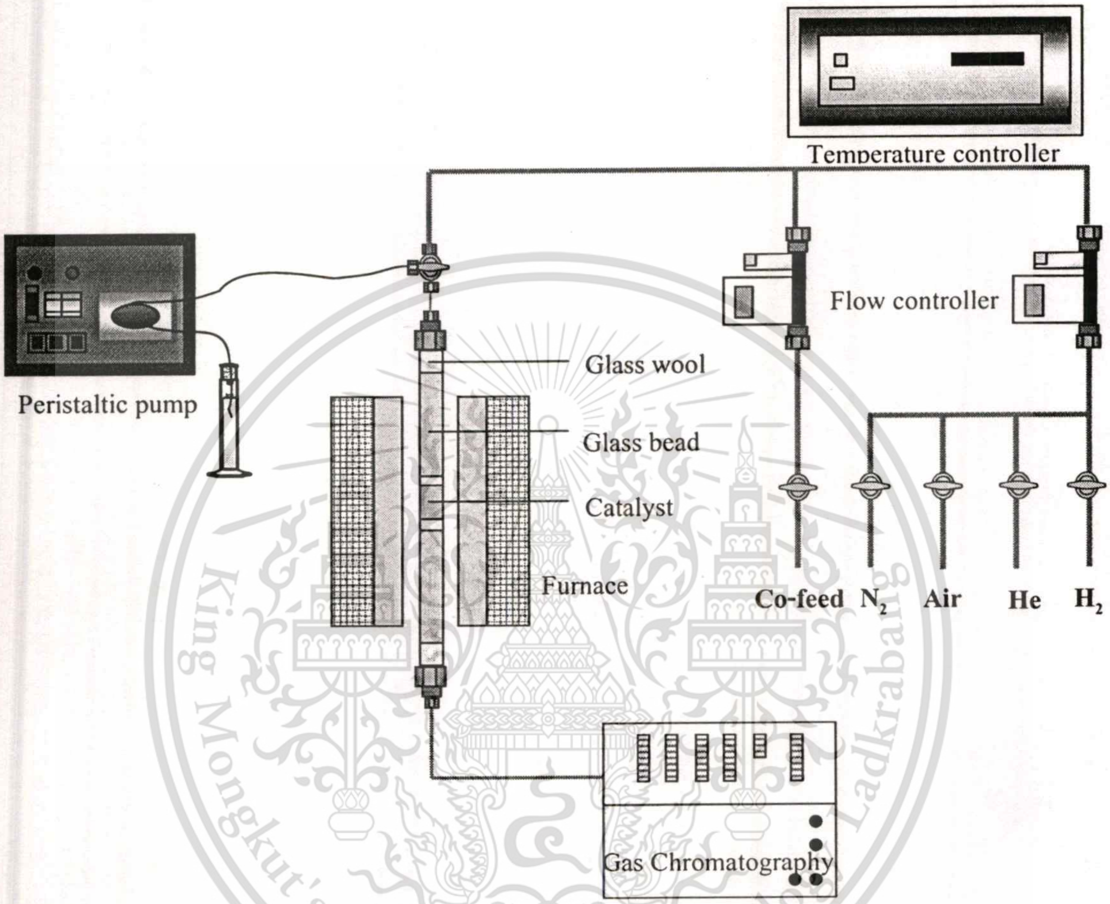

Figure 3.1 The catalytic test rig

The product mixture was analyzed online by gas chromatography equipped with 15 m VA-1 capillary column and flame ionization detector (FID). Product components were analyzed by condition shown in Table 3.2

Table 3.2 Gas Chromatography conditions

Injector Temperature (°C)	Carrier Gas	Column Oven				FID detector temperature (°C)
		Temp. (°C)	Rate (°C/min)	Holding Time (min)	Total Time (min)	
185	He	30	0	5.0	5.0	250
		160	5.0	1.0	32.0	
		200	20.0	11.0	45.0	

The peak area from the chromatogram were measured and calculated as the peak area percentage. Then the unknown peak can be identified using hydrocarbon standard and the composition of product is computed by the normalization method as shown in Appendix A.

CHAPTER 4

RESULTS AND DISCUSSION

4.1 Characterisation of zeolites

4.1.1 X-ray diffraction

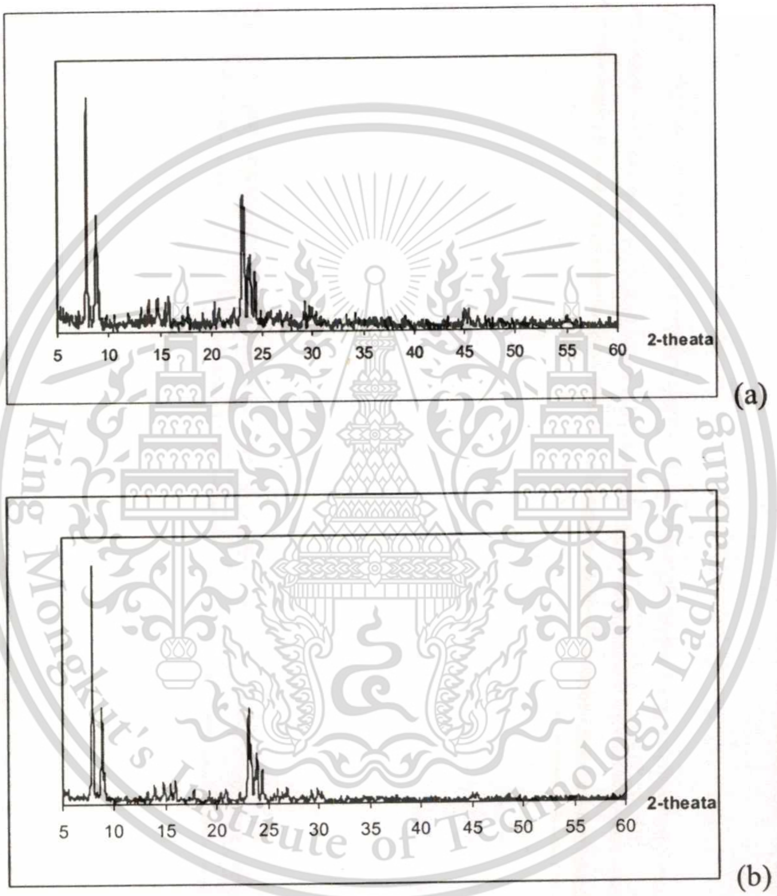

Figure 4.1 X-ray diffraction patterns of (a) HZSM-5 with Si/Al ratio of 11 (HZ11). (b) HZSM-5 with Si/Al ratio of 28 (HZ28).

Catalysts used in this work are zeolites HZSM-5 type (HZ11 and HZ28) and their X-ray diffraction patterns are shown in Figure 4.1. It is shown that structure of both HZSM-5 zeolites are identical to the ZSM-5 standard structure and the crystallinity of the ZSM-5 have been preserved during the calcination process.

4.1.2 Morphology

The electron micrograph of HZSM-5 zeolites are shown in Figure 4.2. The crystallite size of HZ11 (Figure 4.2 a) and HZ28(Figure 4.2 b) is approximately 2.3 μm and 0.52 μm, respectively. Both samples appear to be well define crystalline materials.

(a) (b)

Figure 4.2 Morphology of (a) HZ11. (b) HZ28.

4.1.3 Silver content and Surface area

The chemical composition of HZSM-5 and AgHZSM-5 zeolites were determined by X-ray fluorescence spectroscopy (XRF). From the XRF results, the Si/Al ratio and degree of ion-exchange are calculated as shown in Appendix A. The BET surface area of the zeolites are determined by gas adsorption and presented in Table 4.1.

Table 4.1 The specific surface area of HZSM-5 and AgHZSM-5 catalysts

Si / Al ratio	Ag (%wt)	Degree of ion-exchange (%)	Surface area (m^2/g)
11	-	-	644
	0.7	4.1	623
	1.3	8.9	570
	3.0	20	481
	4.8	33	356
28	-	-	560
	3.0	50	493

The BET surface area of HZ11 and HZ28 zeolite is found to be 644 and 560 m^2/g, respectively. This suggests that they would be effective due to their high surface area. The surface area of both catalysts decreased with increasing silver loading implying channel occupation by incorporated silver species.

4.1.4 Acid site

Acid site in the catalyst has been investigated by using ^1H MAS NMR. The results are shown in Figure 4.3.

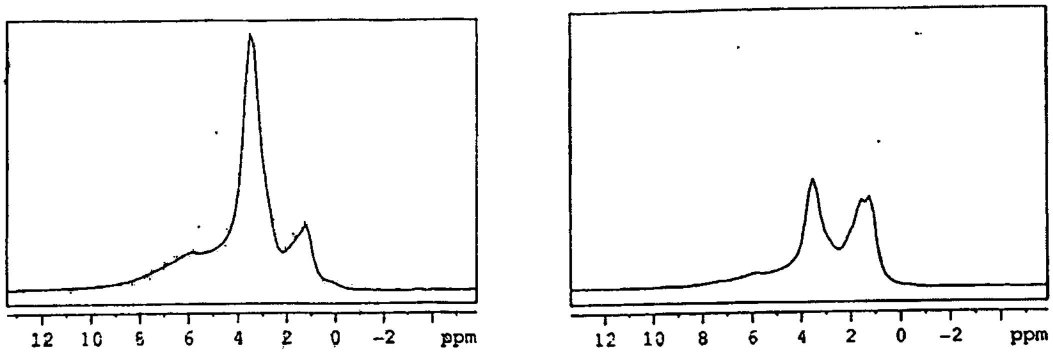

(a)

(b)

Figure 4.3 ^{1}H MAS NMR spectra of (a) HZ11. (b) HZ28.

From ^{1}H MAS NMR spectra of HZ11 (Figure 4.3(a)) and HZ28 (Figure 4.3(b)), there are two main signals at the chemical shift of 1.5 and 3.8 ppm due to terminal silanol groups and bridging hydroxyl groups (Brønsted acid sites), respectively. Relative to the silanol group (peak at 1.5 ppm), intensity of the Brønsted acid sites (peak at 3.8 ppm) of HZ11 was higher than that of HZ28. This indicates the relatively higher Brønsted acid sites in HZ11, as compared to HZ28. This is because HZ11 consists of high aluminium in framework, number of Brønstead acid sites of HZ11 are therefore greater than that in HZ28 which are depicted as below:

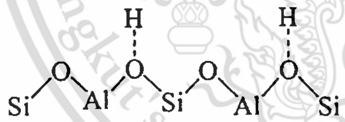

(HZ11)

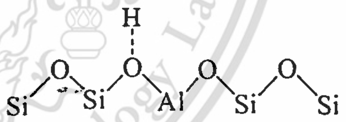

(HZ28)

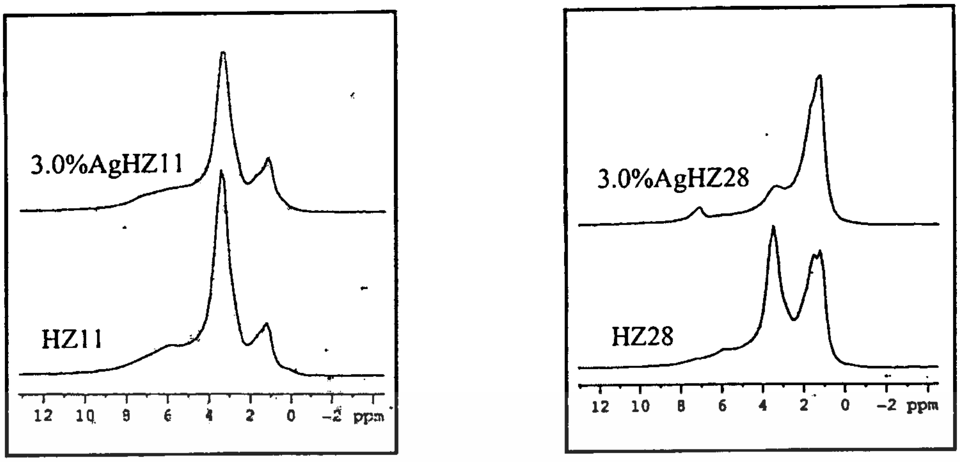

(a) (b)

Figure 4.4 ^{1}H MAS NMR spectra of (a) HZ11 and 3.0%AgHZ11 . (b) HZ28 and 3.0%AgHZ28.

From Figure 4.4, it was found that Brønsted acid site of both silver incorporated HZSM-5 are markedly reduced, as compared to the parent HZSM-5. This is due to the substitution of silver cation on the Brønsted acid sites, as depicted schematically as follow:

4.2 Ethanol conversion over HZSM-5

In all runs, the conversion of ethanol was found to be virtually completed. Similar to other works [4,18,31], it was observed that ethanol was completely converted to hydrocarbons on ZSM-5 catalysts at temperatures higher than 300°C. The product distribution of the reaction obtained over HZ28 is shown in Figure 4.5.

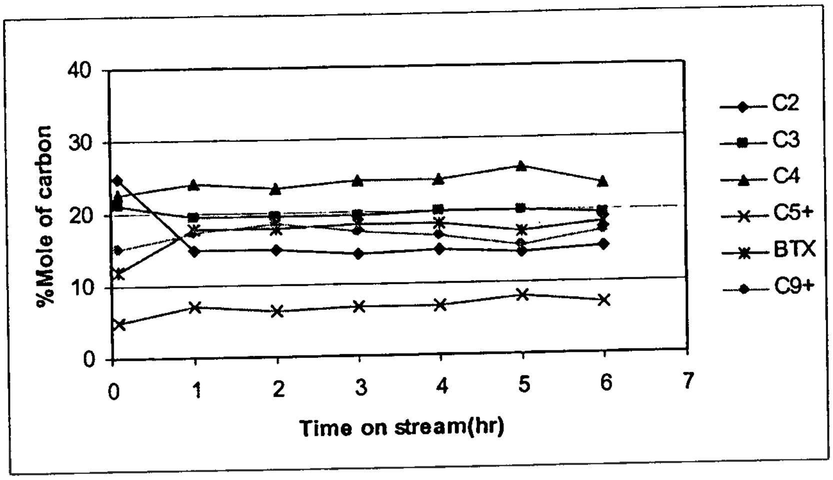

Figure 4.5 Product distribution from ethanol conversion over HZ28 zeolite. *(Reaction temperature; 425°C, W/F; 10.25 g.hr/mol, Carrier gas; nitrogen)*

In mechanistic point of view, ethanol is first dehydrated to ethylene. Ethylene is considered to be the primary product that can oligomerise to from higher olefins which further undergo double bond isomerization, skeletal isomerization, alkylation, cracking, reforming and aromatization to from olefins, paraffins, naphthenes and aromatics. Products formed by these reactions, includes propylene (C3), C4 hydrocarbons, C5-C8 non-aromatic hydrocarbons (C5+), C6-C8 aromatic hydrocarbons (BTX) and high molecular weight hydrocarbons (C9+ which are mainly aromatics [4,18]). The general pathway for the production of various hydrocarbons can be illustrated as below:

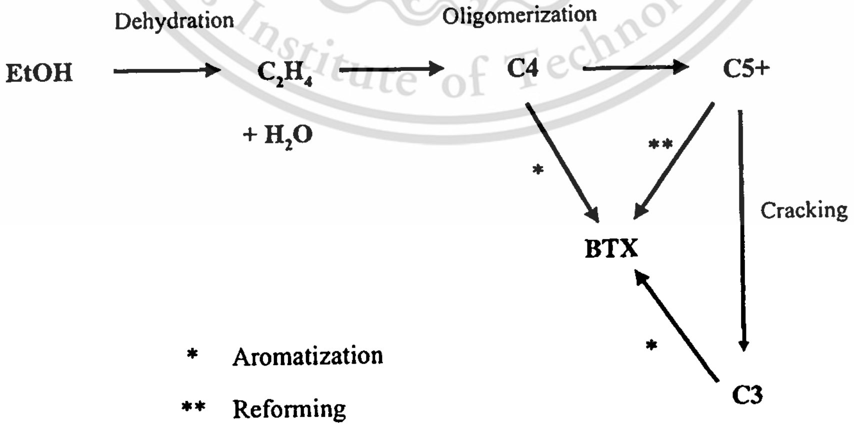

From Figure 4.5, a low catalyst deactivation is observed. The near steady state data can be collected at 2-4 hours on stream and will be used for further discussion.

4.2.1 The effect of W/F over HZSM-5

To investigate the effect of W/F over HZ28 zeolite, a series of reactions were carrier out between W/F of 6.75-27 g.hr/mol at 425°C. The product distribution as a function of W/F are shown in Figure 4.6.

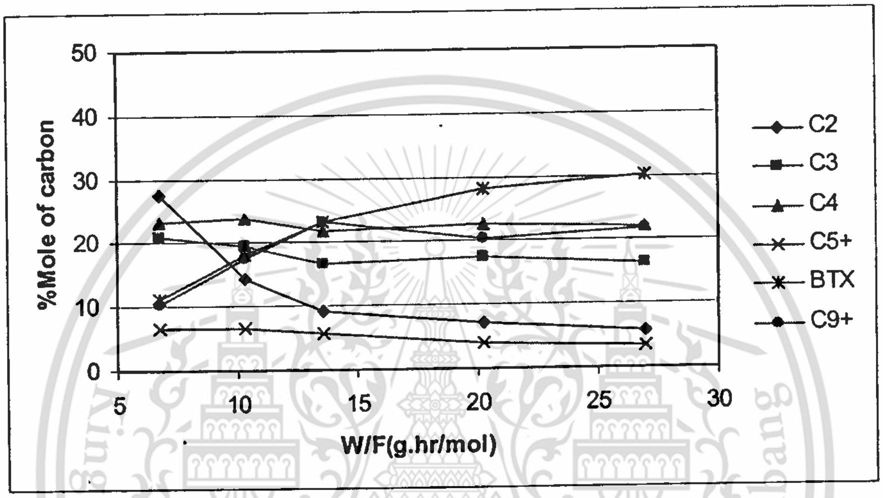

Figure 4.6 W/F-dependence of hydrocarbon distribution over HZ28 zeolite. *(Reaction temperature; 425°C, W/F; 10.25 g.hr/mol, Carrier gas; nitrogen, Average time on stream; 2-4 hours)*

The result in Figure 4.6 show the strong influence of W/F on the product distribution. At low W/F (< 13.5 g.hr/mol), catalytic activity is proportional to the concentration of catalyst (W/F). However at W/F $\geq$ 13.5 g.hr/mol, the activity remain unchange. This is because catalytic activity approaches a limit so called saturation kinetics which is observed frequently in high W/F catalysis. From the result, a low W/F (10.25 g.hr/mol) which can clearly reveal effects from kinetic parameters is chosen in this study.

From Figure 4.6, ethylene is decreased and higher hydrocarbons are increased with increasing W/F which is proportional to the contact time [5,23,29]. W/F seems to be a strong function of the conversion of ethylene to higher hydrocarbons. At low W/F, ethylene can be slightly converted to higher hydrocarbons due to the low rate of ethylene oligomerization. As the W/F is risen, ethylene can react to form oligomers such as C4 and C5+ hydrocarbons which can react further to from various hydrocarbons via reactions that has been shown in the above reaction path way. Consequently, ethylene is decreased and higher hydrocarbons such as BTX are increased with an increase in W/F.

4.2.2 The effect of acidity over HZSM-5

The effect of acidity over HZSM-5 has been investigated using different Si/Al ratio (HZ11 and HZ28). The product distribution of ethanol conversion reveals a dependence on the acidity as shown in Figure 4.7.

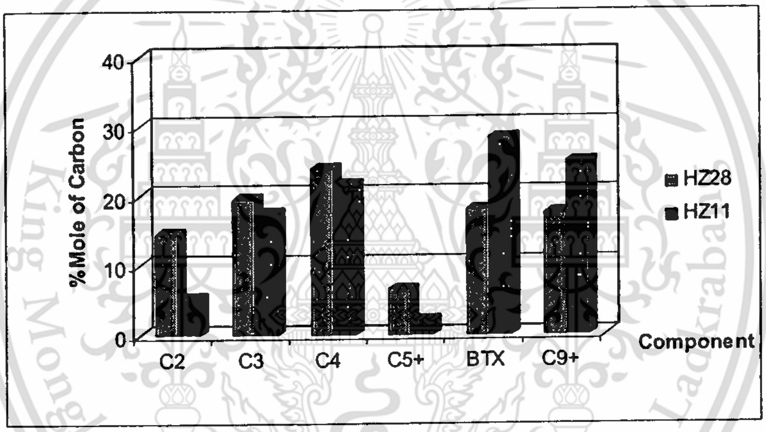

Figure 4.7 Product distribution over HZ11 and HZ28 zeolites. *(Reaction temperature; 425°C, W/F; 10.25 g.hr/mol, Carrier gas; nitrogen, Average time on stream; 2-4 hours)*

It is found that ethylene is decreased with increasing acidity (lower Si/Al ratio) due to the increased in ethylene oligomerization. This is because this reaction proceeds initially via a primary carbocation which occurs on the acid site [12]. When acidity increases, there is sufficient acidity to convert intermediate hydrocarbons, such as ethylene, into higher hydrocarbons [4,18,23,29]. Therefore, over high acidity catalyst, higher hydrocarbon products should be increased. However, it was found that C3, C4 and C5+ hydrocarbons are decreased, as compared to HZ28. It is suggested that C3, C4 and C5+ hydrocarbons could undergo oligomerization, isomerization, dehydrocyclization (Reforming) forming mainly aromatics. This is because these reactions occur via carbocationic processes permitting skeletal rearrangement of alkanes and cycloalkanes [4,12]. Consequently, BTX is produced from hydrocarbons reforming. Thus, it should be noted that as the general rule, catalyst with higher acidity produced more BTX than that with lower acidity.

However, HZSM-5 possesses excellent dehydration, oligomerization and reforming activities but it is a poor dehydrogenation catalyst for small hydrocarbons. Therefore, it requires modification by the addition of metal species. A very recent study [33] showed that AgHZSM-5 is an effective catalyst for the conversion of ethanol to aromatics at 425°C. Therefore, silver is chosen in this study for enhancing dehydrogenation activity of the catalyst.

4.3 Ethanol conversion over AgHZ11

4.3.1 The effect of silver content over HZ11

Effect of silver content for ethylene oligomerization activity from ethanol conversion over silver incorporated HZ11 are shown in Figure 4.8.

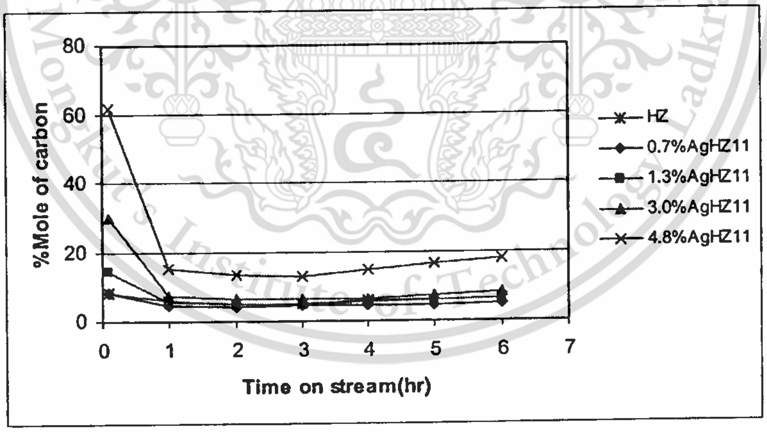

Figure 4.8 Yield of ethylene with time on stream over HZ11 and AgHZ11 zeolite. *(Reaction temperature; 425°C, W/F; 10.25 g.hr/mol, Carrier gas; nitrogen)*

Regarding to the initial conversion, it is found that ethylene oligomerization decreased with increasing silver content. It becomes clear that the concentration of acid site is initially responsible for oligomerization activity. As silver content is increased, the acidity is decreased by substitution of silver cation on exchangeable Brønsted acid sites (HZ11 > 0.7%AgHZ11 > 1.3%AgHZ11 > 3.0%AgHZ11 > 4.8%AgHZ11), as seen by ^{1}H MAS NMR (Figure 4.4). The decrease in acidity would lead to a reduced oligomerization activity accordingly. However, there is no significant change of ethylene oligomerization between 0.7%AgHZ11 and HZ11, indicating that the remaining acid sites in 0.7%AgHZ11 is efficient for ethylene oligomerization. After an hour on stream, it is surprised that the increase in ethylene oligomerization over AgHZ11 is obtained over all catalyst. This indicates that there is relatively high Brønsted acid site, as compared to initial conversion. It is suggested that silver cation could possibly be reduced during the reaction, forming silver metal and bearing consecutive acid sites within the framework. Formation of the silver metal and the recovery acid site are depicted schematically as follow:

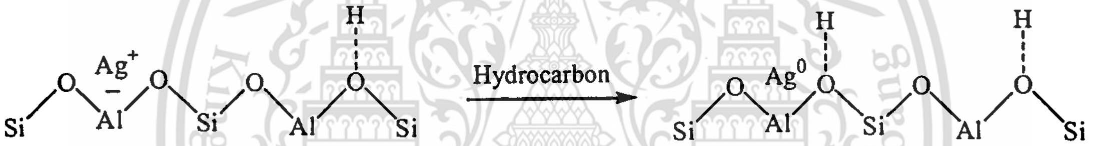

Further evidence support the above suggestion was obtained from ^{1}H MAS NMR spectra (Figure 4.9). It can be seen that when 3.0%AgHZ11 was reduced under H_2 atmosphere at 425°C (red-3.0%AgHZ11), the Brønsted acid site (~ 3.8 ppm) was markedly pronounced. As the acid site is recovered upon the reduction of silver cation, therefore the oligomerization activity is enhanced.

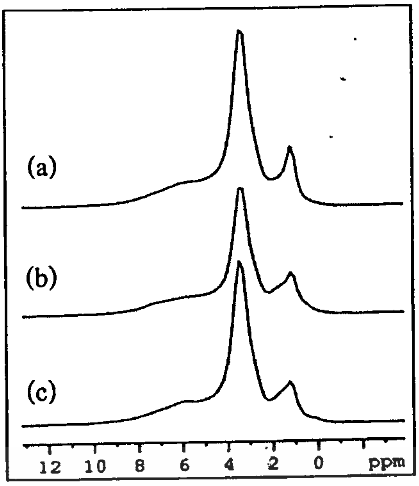

Figure 4.9 ^{1}H MAS NMR spectra of (a) red-3.0%AgHZ11. (b) 3.0%AgHZ11. (c) HZ11.

However, oligomerization activity of 4.8%AgHZ11 was relatively low, as compared to HZ11. This may well be ascribed that at the high silver loading, silver metal particles could agglomerate to silver metal cluster (Ag^0_n) [26,31]. Accordingly, silver metal cluster may partially block the pore of zeolite, leading to low activity for high silver loading zeolite. In fact, the formation of metallic silver particularly over 3.0%AgHZ11 and 4.8%AgHZ11 were confirmed by the X-ray diffraction (XRD) of the catalyst after using.

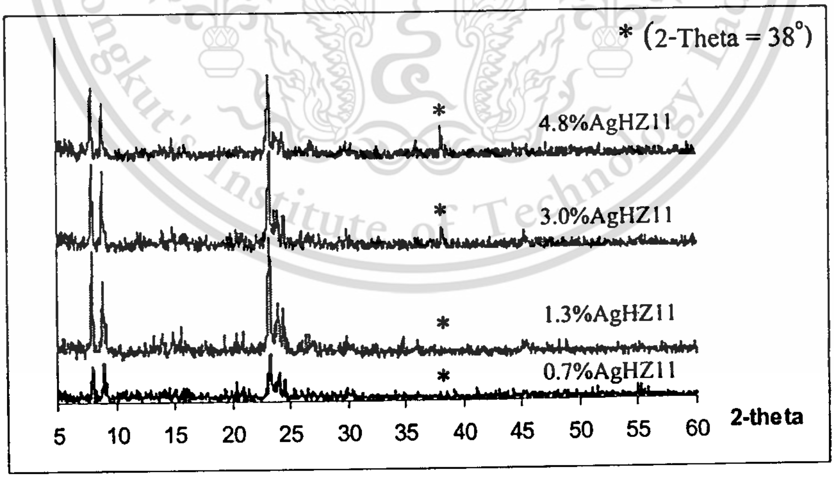

Figure 4.10 XRD pattern of AgHZ11 zeolite after ethanol conversion.

Figure 4.10 shows the XRD patterns of silver catalysts after ethanol conversion for 12 hours. Over high silver loading sample (3.0% and 4.8%AgHZ11), the diffraction peaks for metallic silver at 2θ of 38° were clearly evident. However, for the 0.7 and 1.3 wt.% AgHZ11 samples, no reflect plane due to metallic silver particles were observed, only the diffraction pattern of HZSM-5 zeolite itself were revealed. This is presumably because the reduced silver species is present in small amounts and/or highly dispersed. Therefore, it is not detectable by XRD technique.

Although ethylene oligomerization is not enhanced over AgHZ11, as compared to HZ11, an increase in BTX selectivity is obtained from the reactions using silver loaded AgHZ11 catalysts. The selectivity of BTX over AgHZ11with various silver content at 1 hour after the reaction are plotted in Figure 4.11.

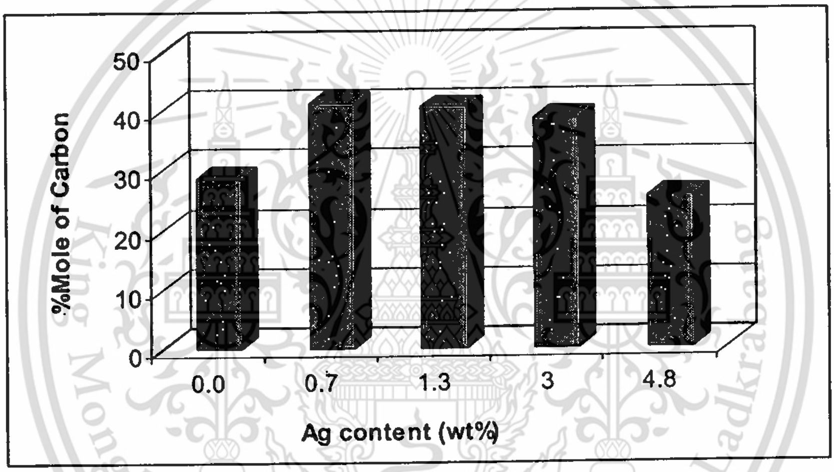

Figure 4.11 Effect of silver content for BTX formation over AgHZ11 zeolite. *(Reaction temperature; 425°C, W/F; 10.25 g.hr/mol, Carrier gas; nitrogen, Time on stream; 1 hour)*

From Figure 4.11, the enhanced aromatics selectivity may well be attribute to the ease of C-H cleavage and the suppress of C-C bond cleavage by loading silver into HZSM-5 [24]. Therefore, the presence of silver in HZSM-5 can promote dehydrogenation of hydrocarbons to aromatics. However, a decreased of BTX with increasing silver content can be observed over AgHZ11. This is not only due to the decreased oligomerization activity, but also the formation of high molecular weight products when silver is present. This is because the excessive silver content in AgHZ11 catalysts will be favorable for the formation of large hydrocarbon molecule deposition on the catalysts, resulting in an increased in the formation of coke. This conclusion is supported by the observed Thermogram of AgHZ11 after the reaction as shown in Figure 4.12.

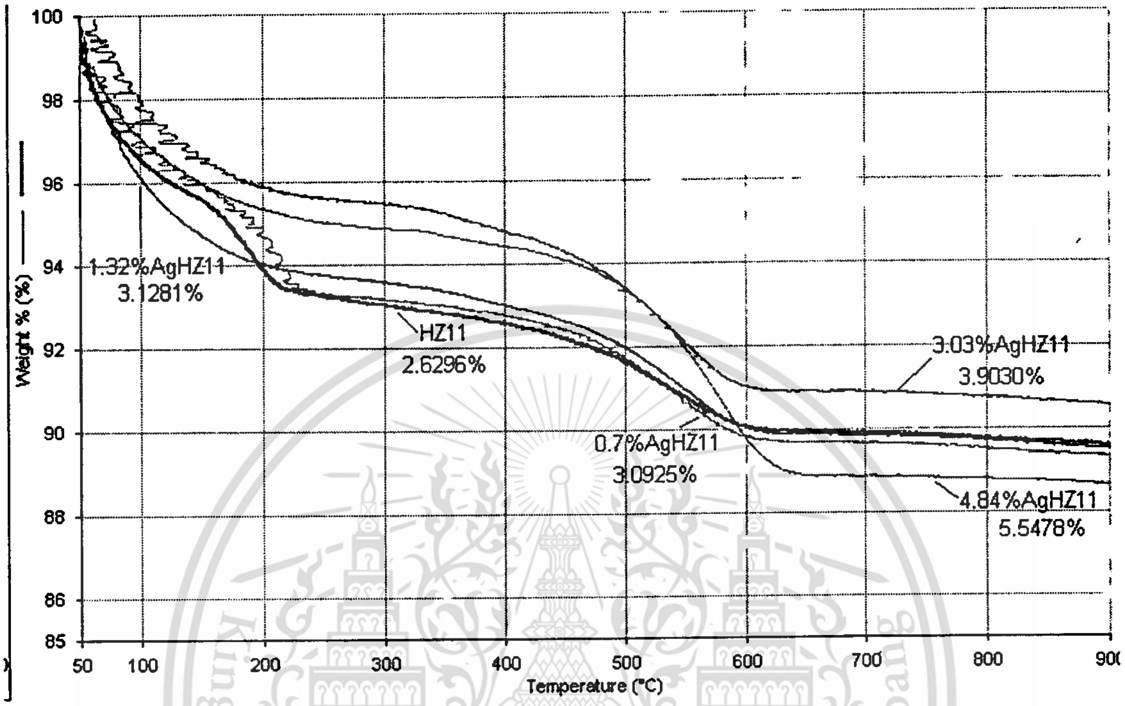

Figure 4.12 Thermogram profiles of the coked AgHZ11 catalysts with various silver content in zeolite .

It can be observed from Figure 4.12 that the order for the amount of coke formed on the AgHZ11 is in the order of 4.8%AgHZ11 (5.5478%) > 3.0%AgHZ11 (3.9030%) > 1.3%AgHZ11 (3.1281%) > 0.7%AgHZ11 (3.0925%) > HZ11 (2.6296%). It becomes clear that the amounts of carbonaceous deposit on AgHZ11 distinctly increased with silver content in zeolite.

4.3.2 The role of silver in product selectivity from ethanol conversion

It is clear that silver incorporated HZ11 can improve BTX formation in ethanol conversion despite ethylene oligomerization is not enhanced. Product selectivity from ethanol conversion over with and without the presence of silver are shown in Figure 4.13.

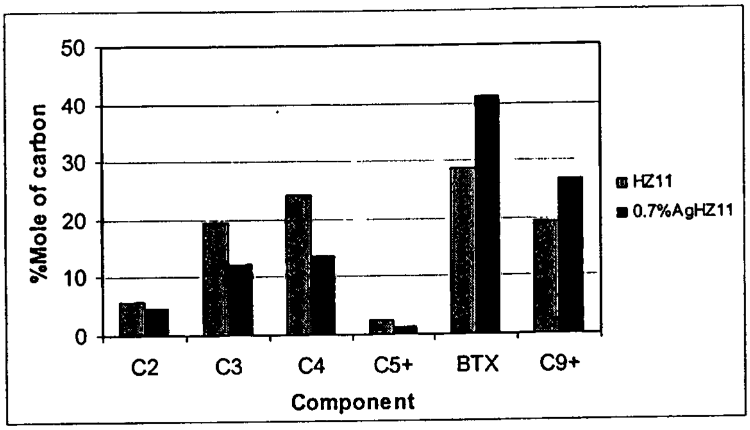

Figure 4.13 Product distribution over HZ11 and 0.7%AgHZ11 zeolite. *(Reaction temperature; 425°C, W/F; 10.25 g.hr/mol, Carrier gas; nitrogen, Time on stream; 1 hour)*

Although, ethylene oligomerization in the reaction using 0.7%AgHZ11 as catalyst is similar to that using HZ11, selectivity of C_3 and C_4 hydrocarbons are exceedingly decreased. This may well be ascribed that the presence of silver species could possibly converted C_3 and C_4 hydrocarbons to aromatics (BTX, C_9^+ hydrocarbons) which consistent with the observed higher aromatic selectivity. This assumption is well agree with the previously report that silver incorporated with HZSM-5 has a high activity for aromatization of light hydrocarbons [24]. Consequently, the observed decrease in C_3 and C_4 hydrocarbons and increase in BTX selectivity in this reaction could only be accounted for aromatization activity of AgHZ11.

4.3.3 The effect of regeneration over AgHZ11

In any case, the carbonaceous deposit on zeolites would decrease catalytic activity by covering the active sites or by blocking the access of reactant molecules to the active sites. Hence, a regeneration was necessary, the catalytic activity and selectivity should be renewed when the deposited coke is burned off. In Figure 4.14(a), after regeneration, the ethylene oligomerization activity of regenerated AgHZ11 (reg-AgHZ11) at low silver content appears to be the same as observed in the fresh catalyst. However, there is significant effect of regeneration for AgHZ11 only at higher silver content (4.8%AgHZ11). It can be seen that ethylene oligomerization over reg-AgHZ11 (4.8%AgHZ11) is higher than the parent catalysts.

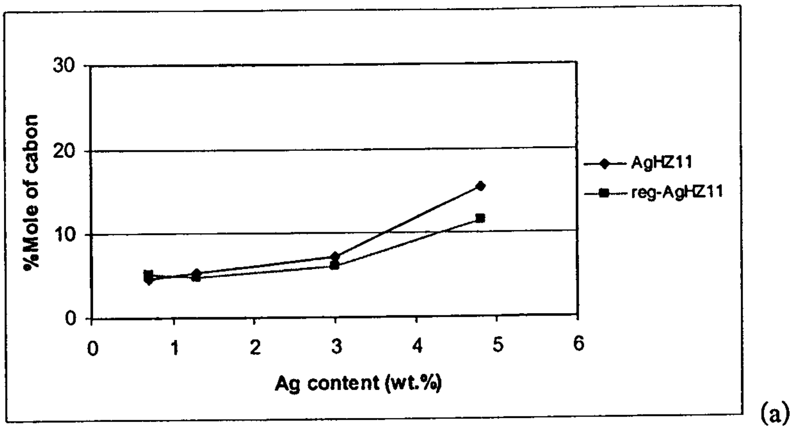

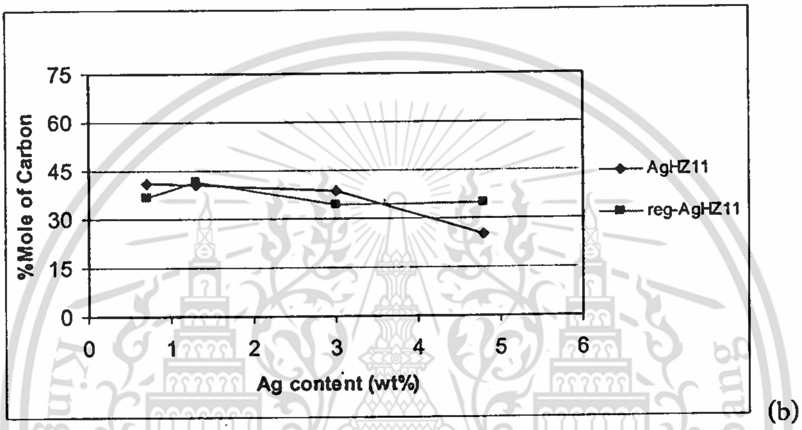

Figure 4.14 Effect of catalyst regeneration at different silver content on (a) ethylene oligomerization activity. (b) BTX formation. *(Reaction temperature; 425°C, W/F; 10.25 g.hr/mol, Carrier gas; nitrogen, Time on stream; 1 hour)*

This can be distributed from the assumption that silver metal species can be partially redispersed during the regeneration, in a manner similar to that observed over Pt/Al_2O_3 [37]. The redispersion of silver species may inhibit agglomeration of the reduced silver metal, as compared to that in the fresh catalyst. Thus, the pore blocking by silver metal cluster in reg-AgHZ11 would be relatively low, as compared to the fresh catalyst. This would result in an increase in ethylene oligomerization over AgHZ11 at high silver content (4.8%AgHZ11), after regeneration. As the ethylene oligomerization over reg-4.8%AgHZ11 is relatively high, as compared to the fresh catalyst, the BTX formation over reg-4.8%AgHZ11 would therefore be higher than the fresh catalyst.

4.4 Ethanol conversion over AgHZ28

Although, a significant increase in the BTX selectivity is obtained from the silver loading HZ11 (Figure 4.11). This is not the case for silver loading HZ28. In the case of ethanol conversion over 3.0%AgHZ28, it is found that BTX formation and ethylene oligomerization are exceedingly low, as compared to HZ28 (Figure 4.15).

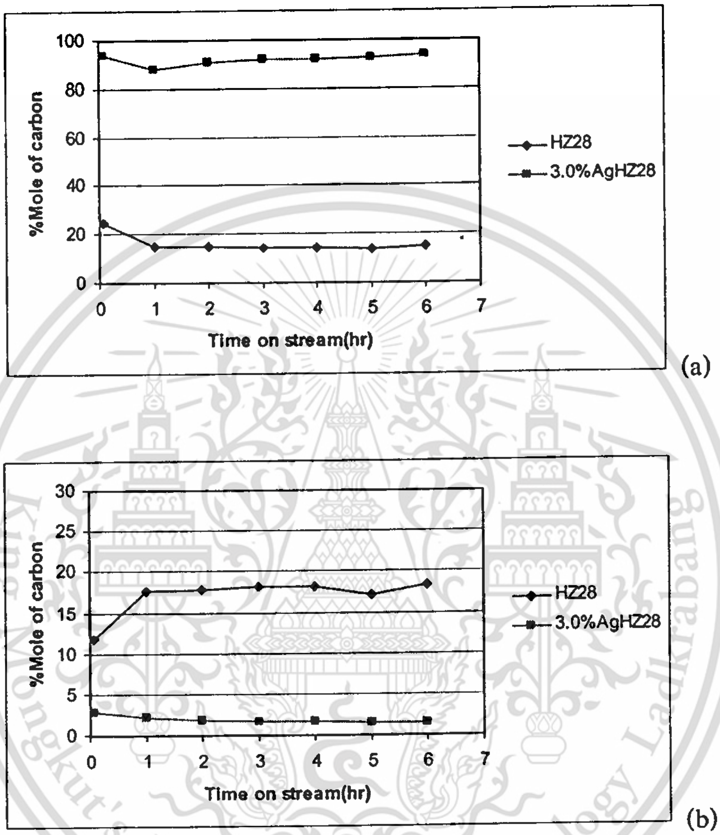

Figure 4.15 Effect of incorporated silver with HZ28 zeolite for (a) ethylene selectivity. (b) BTX selectivity. *(Reaction temperature; 425°C, W/F; 10.25 g.hr/mol, Carrier gas; nitrogen)*

It is well known that the concentration of acid site is responsible for the oligomerization activity particularly in the case of ethylene which initially proceeds via primary carbocation. The reduce in ethylene oligomerization, indicating the lower acid site in 3.0%AgHZ28. It is suggested that

BrØnsted acid sites is not recovered during the reaction due to silver cation in 3.0%AgHZ28 cannot be reduced to silver metal.

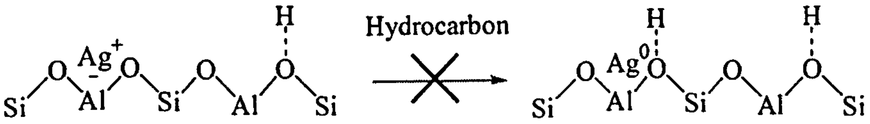

This suggestion is supported by the observed ^{1}H MAS NMR spectra (Figure 4.16) of 3.0%AgHZ28 when it was reduced under H_2 atmosphere at 425 °C. It is found that there is no the increased Brønsted acid sites (Chemical shift ~ 3.8 ppm).

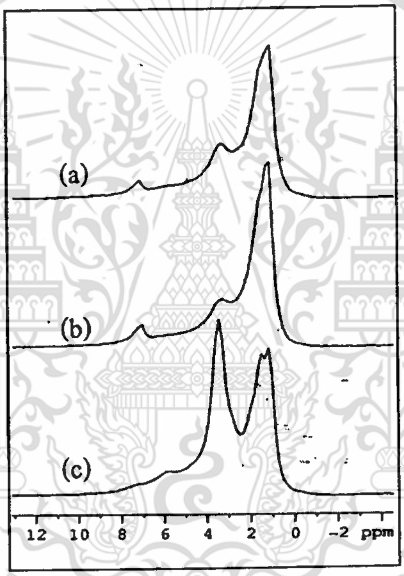

Figure 4.16 ^{1}H MAS NMR spectra of (a) red-3.0%AgHZ28. (b) 3.0%AgHZ28. (c) HZ28.

This is also consistent with the observed XRD pattern of 3.0%AgHZ28 after ethanol conversion (Figure 4.17). It can be seen that no reflect plane due to metallic silver at 2θ of 38° was observed. As silver cation in 3.0%AgHZ28 cannot be reduced during the reaction, no acid site can be obtained. The oligomerization of ethylene for producing high molecular weight hydrocarbon is therefore diminished. As the higher hydrocarbon formation is inhibited, BTX products would therefore decrease, as observed in Figure 4.15 (b).

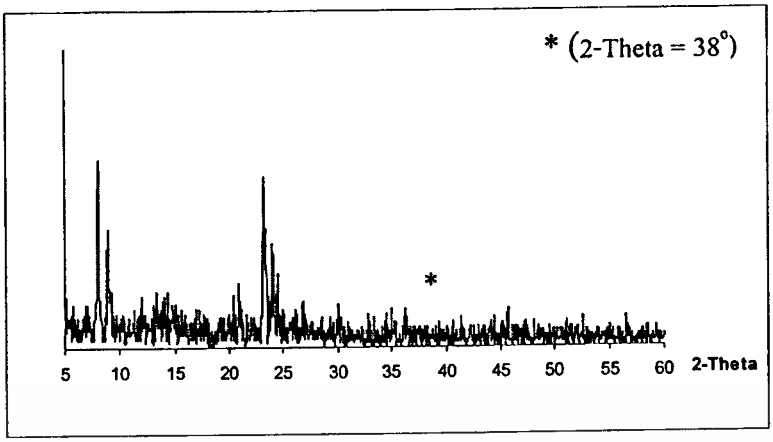

Figure 4.17 XRD pattern of 3.0%AgHZ28 zeolite after ethanol conversion.

From the above result, it can be concluded that 3.0%AgHZ28 is not an appropriate catalyst for ethanol conversion. This is because BrØnsted acid sites cannot be recovered during the reaction over this catalyst, ethylene oligomerization is therefore inhibited.

4.5 Study on reduction of silver in HZSM-5

An interesting observation from the above results is the difference in reduction ability of silver cation species in zeolite with different Si/Al ratio. This inspires the study on the effect of Si/Al ratio on the reduction ability of silver cation species. Although, ^{1}H MAS NMR and XRD suggested that silver cation in 3.0%AgHZ28 cannot be reduced, result from H_2-TPR (Figure 4.18) shows that silver cation species in 3.0%AgHZ28 can be also reduced, but in a manner different from 3.0%AgHZ11.

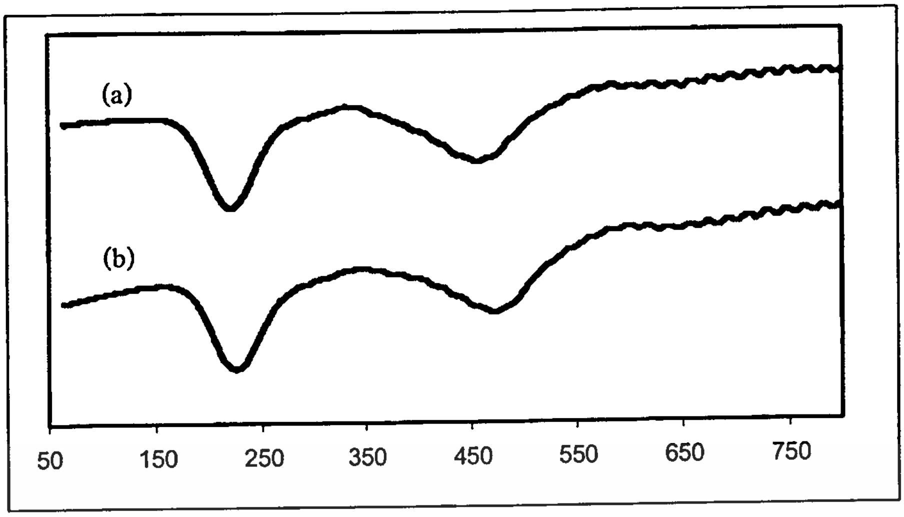

Figure 4.18 H_2-TPR profiles of (a) 3.0%AgHZ11. (b) 3.0%AgHZ28.

Figure 4.18 shows H_2-TPR profiles of silver modified zeolites. For both 3.0%AgHZ11 and 3.0%AgHZ28 samples, there are two H_2 consumption peaks, and the first peak appeared at a temperature range from 150 to 250 °C. The temperature of the second peak is observed from 350 to 600 °C. This is consistent with the previous report suggesting that silver cations are primarily reduced to cationic clusters at low temperature (~100-300°C), and then the cationic clusters can be further reduced into silver metal cluster at high temperature (~365-685 °C). The reduction of silver species are depicted follow :

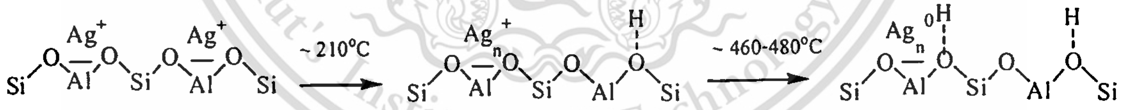

It can be seen from Figure 4.18 that the reduction temperature of the second peak in 3.0%AgHZ28 is shifted to a higher temperature. This indicates that silver cationic cluster in 3.0%AgHZ28 is more difficult to be reduced to silver metal cluster, as compared to that of 3.0%AgHZ11. Hence, there are two possibility for the observed no activity over 3.0%AgHZ28 (section 4.4). (i) As silver cation species in 3.0%AgHZ28 is relatively more difficult to be reduced, the reduction of this species by ethanol, ethylene or hydrocarbon in reaction stream may not take placed or (ii) it is also possible that silver cation in 3.0%AgHZ28 can be reduced into silver metal but it may well react with BrØnsted acid sites back into H_2 and cationic silver species (reversible interconversion). This was previously observed by other reports [26,34-36]. The reversible interconversion is depicted schematically as follow:

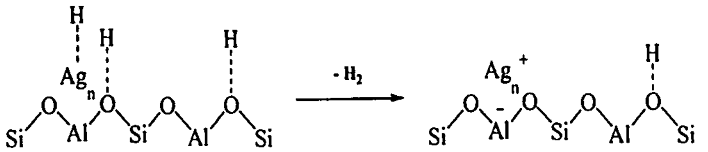

----(1)

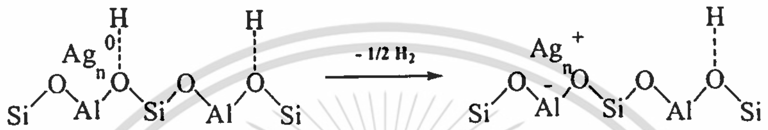

----(2)

There are two hypotheses for the reversible interconversion: (i) H_2 can be readily chemisorbed on the reduced silver species and consecutively dissociate to form hydride. The hydride can readily react with BrØnsted acid sites forming H_2 and silver cation species [26,34-35] or (ii) the reduced silver metal can directly react with BrØnsted acid site to form H_2 and silver cation species in a manner similar to ZnZSM-5 observed in literature [36].

Additionally, the loss of BrØnsted acid site in 3.0%AgHZ28 which is contributed from the reversible interconversion can be confirmed by TPHE technique, as shown in Figure 4.19.

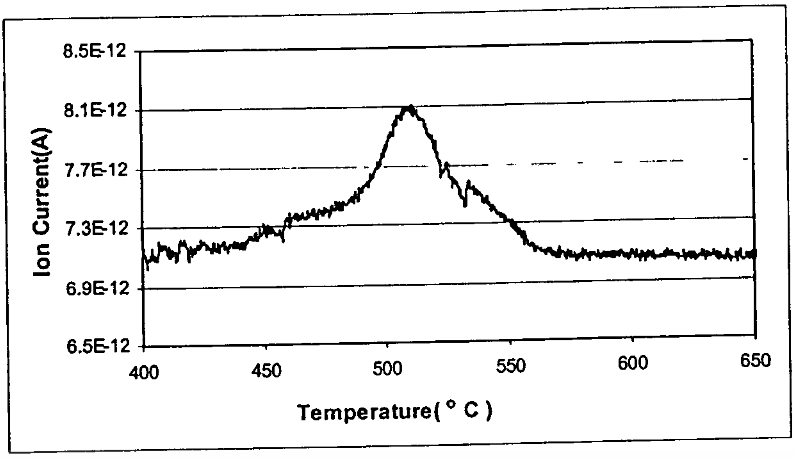

Figure 4.19 TPHE curve of red-3.0%AgHZ28.

It was shown that the hydrogen gas can be released from red-3.0%AgHZ28 upon heating in an inert gas stream. This confirms the reversible interconversion of incorporated silver metal and Brønsted acid sites to give H_2 at temperature 450-570 °C.

Further evidence support the above suggestion was obtained by the secondary H_2-TPR results (Figure 4.20) of 3.0%AgHZ11 and 3.0%AgHZ28 when they were reduced again after the first reduction.

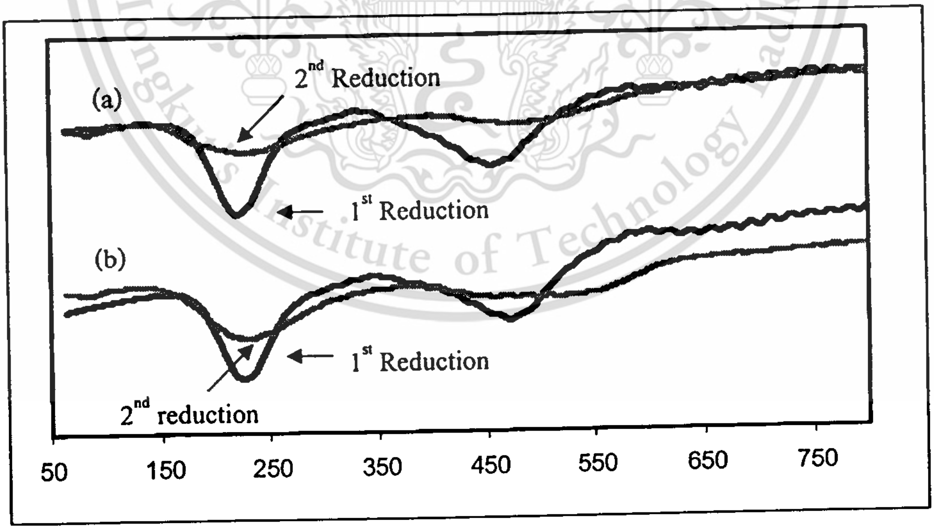

Figure 4.20 Secondary H_2-TPR profiles of (a) 3.0%AgHZ11. (b) 3.0%AgHZ28.

Surprisingly, both sample can be repeatedly reduced despite they were not exposed to atmosphere. This indicates the reversible interconversion of reduced silver metal and BrØnsted acid sites into silver cation species and H_2, at high temperature. In addition, it can be seen that the difference in H_2 consumption peaks between the 1st and 2nd reduction of 3.0%AgHZ28 is less than that of 3.0%AgHZ11. It is suggested that the reversible interconversion of reduced silver metal in 3.0%AgHZ28 can be more feasible than that in 3.0%AgHZ11. Therefore, the amount of H_2 used for 2nd reduction of silver cation species to silver metal species in 3.0%AgHZ28 is higher than that in 3.0%AgHZ11.

According to the above evidences, it is believed that the observed different activity of silver in 3.0%AgHZ11 and 3.0%AgHZ28 may be arised from the different in their reversible interconversion activity. In 3%AgHZ11, the site proximity is relatively close, the reduced silver metal can be easily agglomerated into large silver metal cluster (as seen in XRD after ethanol conversion over AgHZ11) which is difficult to undergo reversible interconversion with BrØnsted acid sites. On the other hand, the reduced silver metal in 3.0%AgHZ28 is not stable. Therefore, the reversible interconversion of the reduced silver metal in 3.0%AgHZ28 would be more feasible than that in 3.0%AgHZ11.

In thermodynamic point of view, the reversible interconversion of reduced silver metal and BrØnsted acid sites can be suppressed in the presence of H_2. Moreover, the presence of H_2 may well lead to the ease of silver cation species reduction. Accordingly, it is suggested that the presence of H_2 would probably increase activity of the reaction using 3.0%AgHZ28 as catalyst. This is indeed observed in the reaction of ethanol conversion using 26%H_2/N_2 as carrier gas, as in Figure 4.21. It is shown that the ethylene oligomerization activity of 3.0%AgHZ28 was enhanced in the presence of H_2, as compared to that without H_2 (Figure 4.21(a)). This indicates that the acid site of 3.0%AgHZ28 is pronounced in the presence of hydrogen. This may well be ascribed that the continuous feeding of H_2 keeps the silver species in a reduced form or it can reduce silver cation species to silver metal species, bearing consecutive BrØnsted acid sites. As the acidity is pronounced upon the reduction of silver cations, the oligomerization is therefore facilitated.

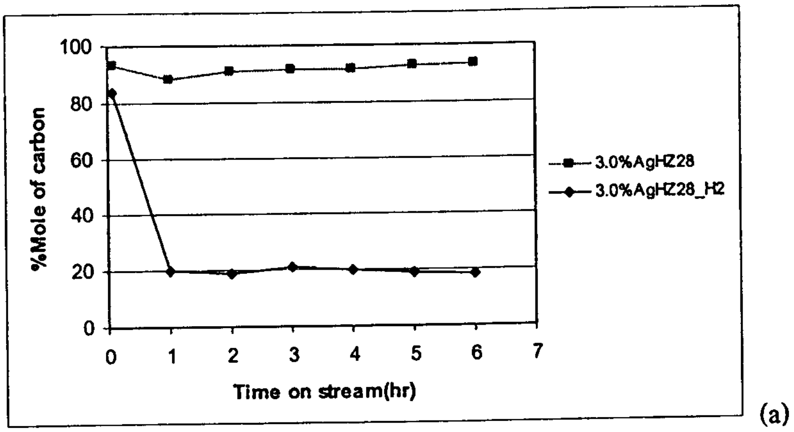

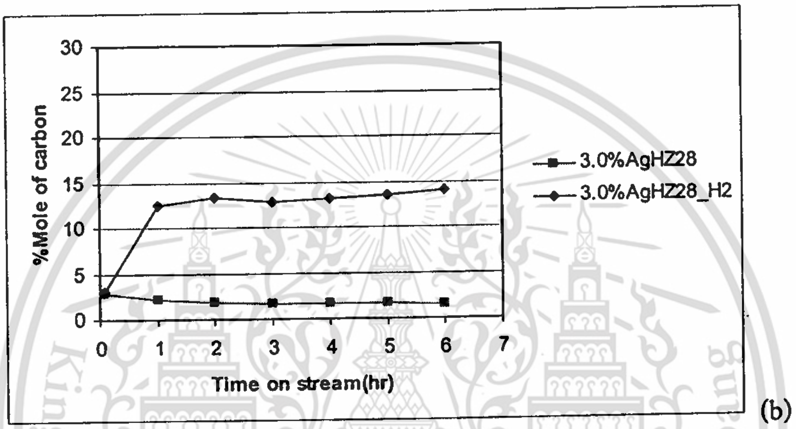

Figure 4.21 Effect of co-feeding H_2 over 3.0%AgHZ28 for (a) ethylene oligomerization. (b) BTX formation. *(Reaction temperature; 425°C, W/F; 10.25 g.hr/mol, Carrier gas; 26% hydrogen in nitrogen)*

This suggestion is supported by the observed XRD pattern of 3.0%AgHZ28 after ethanol conversion in the presence of 26%H_2/N_2 (Figure 4.22). It can be seen that additional reflect plane due to the metallic silver cluster is revealed at 2θ of 38°.

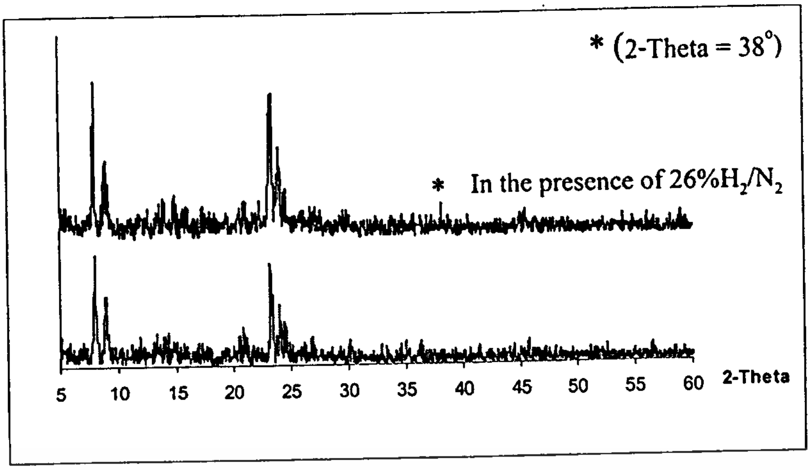

Figure 4.22 XRD pattern of 3.0%AgHZ28 zeolite after ethanol conversion.

Regarding to the formation of metallic silver cluster, this may well be described that silver cation can be reduced by H_2 or silver is kept in reduced form by continuous feeding of H_2. Consequently, reduced silver metal has an opportunity to agglomeration to large silver metal cluster. Therefore, the reflect plane due to silver metal cluster can be observed in XRD pattern of 3.0%AgHZ28 after ethanol conversion in the presence of H_2.

Since, ethylene oligomerization activity of 3.0%AgHZ28 is promoted in presence of H_2, the increase in BTX selectivity can be observed in Figure 4.21(b).

From the above result, ethylene oligomerization is an important step for the ethanol conversion and a balance between oligomerization and dehydrogenation activity is essential for obtaining high yield of aromatics.

CHAPTER 5

CONCLUSION AND SUGGESTIONS

5.1 Conclusion

In the reaction using HZSM-5, ethylene oligomerization is important for the production of higher hydrocarbons and aromatics. The experiments show the strong influence of W/F and acidity in HZSM-5 on the product distribution. When W/F is risen, ethylene can further react to form higher hydrocarbons. Over high acidity catalyst, ethylene oligomerization is enhanced because this reaction proceeds initially via primary carbocation which occurs on the acid site. Therefore, the acidity is essential for the ethylene oligomerization to higher hydrocarbons and aromatics.

The incorporation of silver into HZSM-5 (11) zeolite appreciably enhances the aromatization activity of light hydrocarbons to aromatics (BTX and C9+). The highest selectivity of aromatics is obtained with the low silver-exchanged zeolite (0.7%AgHZ11) and BTX is decreased with increasing silver content. This is not only due to the decreased oligomerization activity by silver species, but also to the fact that the excessive silver content in AgHZ11 catalyst facilitates the formation of large hydrocarbon molecule deposited on the catalyst, resulting in a rapid deactivation.

After catalyst regeneration, the redispersion of silver metal species can reduce the pore blocking of zeolite and consequently enhance the ethylene oligomerization. Therefore, the regeneration may well enhance activity of the catalyst at high silver content.

There is the difference in hydrogen reduction ability of silver cation species in zeolite with different Si/Al ratio. The silver cation species in 3.0%AgHZ28 is more difficult to be reduced to silver metal cluster, as compared to 3.0%AgHZ11. Moreover, the reduced silver metal species in 3.0%AgHZ28 is not stable and may undergo reversible interconversion with Brønsted acid sites to form silver cation species and hydrogen. Whilst reduced silver metal in 3.0%AgHZ11 can be easily agglomerated which is difficult to undergo reversible interconversion. Accordingly, the reduction of silver cation species in 3.0%AgHZ28 by reaction stream may not be take placed or it is possible to be reduced but it may undergo reversible interconversion. Therefore, the Brønsted acid sites of

3.0%AgHZ28 cannot be recovered during the reaction. Hence, ethylene oligomerization and BTX formation in the reaction using 3.0%AgHZ28 are exceeding low.

The presence of hydrogen can enhance the ethylene oligomerization activity and BTX formation in the reaction using 3.0%AgHZ28. This may be because hydrogen can reduce silver cation species to silver metal species or the continuous feeding of hydrogen can keep the silver species in a reduced form, bearing consecutive Brønsted acid sites.

5.2 Suggestions

1. The agglomeration of silver can reduce ethylene oligomerization activity by blocked pore of zeolite. Thus, the mixture of silver with other metal which having similar activity as silver should be studied for diminishing agglomeration of silver.
2. The formation of high molecular weight products when silver is present lead to a rapid deactivation of catalysts. Thus, the low W/F over silver containing HZSM-5 catalysts should be studied for improvement of the catalyst stability.

REFERENCES

[1] M.O. Adebajo., M.A. Long. "The contribution of methanol-to-aromatics reaction to benzene methylation over ZSM-5 catalysts." **Catalysis Communications**, vol. 4, 2003. pp. 71- 76.

[2] H.A. Zaidi., K.K. Pant. "Catalytic conversion of methanol to gasoline range hydrocarbons." **Catalysis Today**, vol. 96, 2004. pp. 155-160.

[3] R. Le Van Mao., P. Levesque., G. Mclaughlin. and L.H. Dao. "Ethylene from ethanol over zeolite catalyst." **Applied Catalysis**, vol. 34, 1987. pp. 163-179.

[4] A.K. Talukdar., K.G. Bhattacharyya. and S. Sivasanker. "HZSM-5 catalysed conversion of aqueous ethanol to hydrocarbons." **Applied Catalysis A: General**, vol.148, 1997. pp. 357-371

[5] Y. Inoue., K. Nakashiro. and Y. Ono. "Selective conversion of methanol into aromatic hydrocarbons over silver-exchanged ZSM-5 zeolites." **Microporous Materials**, vol. 4, 1995. pp. 379-383.

[6] I.M. Campell. **Biomass Catalysts and Liquid fuel.** Pensylvania : Holt Rinehart and Winston. 1983

[7] A.E. Wheals., L.C. Basso., D.M.G. Alves. and H.V. Amorim. "Fuel ethanol after 25 years." **Trends in Biotechnology**, vol. 17, 1999. pp. 482-487.

[8] W. Hsieha., R. Chenb., T. Wub. and T. Lina. "Engine performance and pollutant emission of an SI engine using ethanol–gasoline blended fuels." **Atmospheric Environment**, vol. 36, 2002. pp. 403–410.

[9] J.R. Mielenz., "Ethanol production from biomass: technology and commercialization status." **Current Opinion in Microbiology**, vol. 4, 2001. pp. 324-329.

[10] M.A.S. Al-Baghdadi. "Hydrogen–ethanol blending as an alternative fuel of spark ignition engines." **Renewable Energy**, vol. 28, 2003. pp. 1471–1478.

[11] B. He., J. Wang., J.Hao., X.Yan. and J. Xiao. "A study on emission characteristics of an EFI engine with ethanol blended gasoline fuels." **Atmospheric Environment**, vol. 37, 2003. pp. 949–957.

[12] G.A. Olah., A.Molnar. **Hydrocarbon Chemistry**. Cannada : John Wiley&Sons. 2003.

[13] S.M. Auerbach., K.A. Carrado. and P.K. Dutta, Editors. **Handbook of zeolite science and technology**. New York : Marcel Dekker. 2003.

[14] A. Dyer. **An introduction to zeolite molecular sieves.** New York : John Wiley&Sons. 1998.

[15] B.C. Gates. **Catalytic Chemistry**. New York : John Wiley&Sons. 1992.

[16] S.Bhatia. **Zeolite catalysis: principles and applications.** Florida : CRC Press. 2000.

[17] J.Hagen. **Industrial Catalysis.** Weinheim : WILEY-VCH. 1999.

[18] B. Viswanathan, Editor. **Recent Developments in Catalysis**. New Delhi : Narosa. 1992.

[19] B.Lui., Y. Yang. and A. Sayari. "Non-oxidative dehydroaromatization of methane over Ga-promoted Mo/HZSM-5-based catalysts." **Applied Catalysis A: General**, vol. 214, 2001. pp. 95- 102.

[20] N. Janjic., M.S. Scurrell. "Evidence for the enhancement of the catalytic action of Zn-ZSM-5-based catalysts for propane aromatization using microvawe radiation." **Catalysis Communications**, vol. 3, 2002. pp. 253-256.

[21] N. Viswanadham., G. Muralidhar. and T.S.R. Prasada Rao. "Cracking and aromatization properties of some metal modified ZSM-5 catalysts for light alkane conversions." **Journal of Molecular Catalysis A : Chemical**, vol. 223, 2004. pp. 269-274.

[22] Y. Nagamori., M. Kawase. "Converting light hydrocarbons containing olefins to aromatics (Alpha process)." **Microporous and Mesoporous Materials**, vol. 21, 1998. pp. 439-445.

[23] V.R. Choudhary., P. Devadas., S. Banerjee. And A.K. Kinaage. "Aromatization of dilute ethylene over Ga-modified ZSM-5 type zeolite catalysts." **Microporous and Mesoporous Materials**, vol. 47, 2001. pp. 253-267.

[24] Y. Ono., K. Osako., G-J. Kim. and Y. Inoue. "Ag-ZSM-5 as a catalyst for aromatization of alkanes, alkenes and methanol." **Zeolites and Related Microporous Materials: State of the Art 1994 Studies in surface Science and Catalysis**, vol. 84, 1994. pp. 1773-1780.

[25] C. Shi., M. Cheng., Z. Qu., X. Yang. and X. Bao. "On the selectivity catalytic reduction of No_x with methane over Ag-ZSM-5 catalysts." **Applied Catalysis B:Environmental**, vol. 36, 2002. pp.173-182.

[26] C. Shi., M. Cheng., Z. Qu., X. Yang. and X. Bao. "Investigation on the catalytic roles of silver species in the selective catalytic reduction of NO$_x$ with methane" **Applied Catalysis B: Environmental**, vol. 51, 2004. pp. 171-181.

[27] C.Shi., M. Cheng., Z. Qu., X. Yang. and X. Bao. "On the correlation between microstructural changes of Ag-H-ZSM-5 catalysts and their catalytic performances in the selective catalytic reduction of NO*x* by methane." **Journal of Molecular Catalysis A: Chemical**, vol. 235, 2005. pp. 35–43.

[28] J. Shibata., Y. Takada., A. Shichi., S. Satokawa., A. Satsuma. and T. Hattori. "Influence of zeolite support on activity enhancement by addition of hydrogen for SCR of NO by propane over Ag-zeolites." **Applied Catalysis B: Environmental**, vol. 54, 2004. pp.137-144.

[29] V.R. Choudhary., S. Banerjee. and D. Panjala. "Product distribution in the aromatization of dilute ethylene over H-GaAlMFI zeolite: effect of space velocity." **Microporous and Mesoporous Materials**, vol. 51, 2002. pp. 203-210.

[30] X. Zhu., S. Liu., Y. Song. and L. Xu. "Catalytic cracking of C4 alkenes to propene snd ethane: Influences of zeolites pore structures and Si/Al$_2$ ratios." **Applied Catalysis A: General** , vol. 288, 2005. pp. 134-142.

[31] J. Shibata., K. Shimizu., Y. Takada., A. Shichi., H. Yoshida., S. Satokawa., A. Satsuma. and T. Hattori. "Structure of active Ag clusters in Ag zeolites for SCR of NO by propane in the presence of hydrogen." **Journal of catalysis**, vol. 227, 2004. pp. 367-374.

[32] A.T. Aguayo., A.G.Gayubo., A. Atutxa., B.Valle. and J.Bilbao. "Regeneration of a HZSM-5 zeolite catalyst deactivated in the transformation of aqueous ethanol inti hydrocarbons." **Catalysis Today**, vol. 107-108, 2005. pp. 410-416.

[33] A. Ausavasukhi. The Production of Gasoline and Aromatics from ethanol, MS.D. Thesis of chemistry, Faculty of science, King Mongkut's Institute of Technology Ladkrabang.

[34] T. Baba., H. Sawada. and T. Takahashi. "Chemisorption study of hydrogen and methane by 1H MAS NMR and conversion of methane in the presence of ethylene on Ag-Y zeolite." **Applied Catalysis A: General**, vol. 231, 2002. pp. 55-63.

[35] J.M.A. Lins. and M.A.C. Nascimento. "A density functional study of some silver cluster hydrides." **Chemical physics letters**, vol. 391, 2004. pp. 9-15.

[36] J. Heemsoth., E.Tegeler., F.Roessner and A. Hagen. "Generation of activesites for ethane aromatization in ZSM-5 zeolites by a solid-state reaction of zinc metal with BrØnstead acid sites of the zeolite." **Microporous and Mesoporous Materials**, vol. 46, 2001. pp. 185-190.

[37] F. C. Galisteo., R.Masical., M.L. Granados., J.L.G. Fierro., R.A. Daley. And J.A. Anderson. "Reactivation of sintered Pt/Al2O3 oxidation catalysts" **Microporous and Mesoporous Materials**, vol. 46, 2001. pp. 185-190.

[38] D.A. Skoog., J. J. Leary. **Principles of Instrumental Analysis.** 4th Ed. Philadelphia : Harcourt Brace College. 1992.

APPENDIX A

CALCULATION

A1 Calculation of chemical composition in zeolite samples

The chemical composition of zeolite samples are determined by X-ray fluorescence spectroscopy (XRF). The data from XRF of 0.7%AgHZ11 is shown in Table A1.

Table A1 Data from XRF, calculations of chemical composition of 0.7%AgHZ11

Al_2O_3	SiO_2	Ag
7.10 wt.%	92.1 wt. %	0.702 wt.%

A1.1 Calculation of Si/Al ratio

Mole of SiO_2 in 100 g of sample = [92.10/60.07]

= 1.53

Mole of Al_2O_3 in 100g of sample = [7.10/101.93]

= 0.07

From the above result, the silicon/aluminium ratio is calculated as follows:

Mole of Si = 1.53

Mole of Al = [0.07*2]

Thus; Si/Al = [1.53]/ [0.07*2]

= 10.93

The unit cell of zeolite is calculated as follows:

The general unit cell of HZSM-5 is $H_nAl_nSi_{96-n}O_{192}$

Thus; Si + Al = 96 [Eq.1]

Si/Al = 10.93 [Eq.2]

From Eq.1 and Eq.2

$$\mathrm{Si} = 86.3$$

$$\mathrm{Al} = 9.7$$

From the above, the unit cell of AgHZSM-5 is therefore $Ag_nH_{9.7-n}Al_{9.7}\,Si_{86}O_{192}$. The degree of silver ion-exchange in unit cell of 0.7%AgHZ11 is calculated as follow:

The weight of unit cell, U of 0.7%AgHZ11($Ag_nH_{9.7-n}Al_{9.7}\,Si_{86}O_{192}$)

$$U = n[Ag] + (9.7-n)[H] + 9.7[Al] + 86[Si] + 192[O]$$

$$= 107.87n + (9.7-n) + 261.9 + 2408 + 3072 \qquad [Eq.1]$$

The silver content loaded zeolite sample is

$$[107.87n/U] = [0.7/100] \qquad [Eq.2]$$

From the Eq.1 and Eq.2,

n = 0.4 and hence the unit cell of 0.7%AgHZ11 is $Ag_{0.4}H_{9.3}Al_{9.7}\,Si_{86}O_{192}$. The ion exchange of silver into the exchangeable site of the framework is estimated to be 4.12%.

A3 Catalytic parameter

W/F = [Weight of catalyst (g)/Mole of liquid reactant feed (mol/h)]

In the reaction using 0.01 mol/hour of ethanol feed as feed and using 0.0675 gram of catalyst, the W/F is calculated as follow:

W/F = [0.0675 (g)/0.01(mol/hr)]

= 6.75 g.hr/mol

In a similar manner; W/F of catalysts 0.1025, 0.135, 0.2025, and 0.270 g at constant feed are 10.25, 13.50, 20.25, and 27.00 g.hr/mol, respectively.

A4 Calculation of % mole of carbon from gas chromatography

From the chromatogram, the peaks of hydrocarbon sample were identified using of reference standard for comparison. The peak area of hydrocarbon which possesses the equal number of carbon was summerized. The summerized peak area data which is obtained from chromatogram of a mixture hydrocarbon product is shown in Table A2.

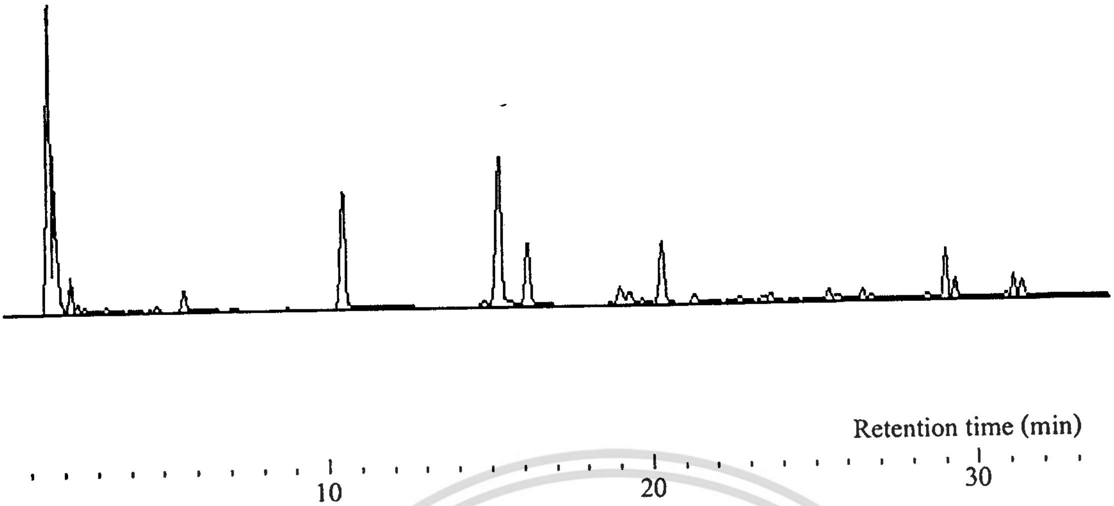

Figure A2 Chromatogram of hydrocarbon product standard.

Table A2 The summarized peak area of a mixture hydrocarbon product.

Number of carbon	Retention time(min)	Summarized area
C_2	1.40-1.48	343.12
C_3	1.49-1.59	888.76
C_4	1.60-2.30	999.21
C_5	2.31-3.00	21.97
C_6	3.01-5.45	53.83
C_7	5.94-10.15	128.21
C_8	10.54-14.53	0.00
B	5.46-5.93	912.00
T	10.15-10.53	28.18
X	14.54-16.63	1970.74
C_9	16.64-45.00	1959.13
Total	-	7305.18

In the normalization method, the areas of all eluted peak were computed; after correcting these areas for differences in the detector response to different compound. In this study, the flame ionization detector (FID) was used because for hydrocarbon it responded proportionally to the number of carbon atoms in the molecule entering the detector per unit time [38]. After summarizing, the carbon fraction of the analyte was obtained from the ratio of its area to the total area of all peaks.

Calculate the carbon mole percent of each component in sample as follow:

$$\text{Carbon mole \% of } C_n = [\text{ Area of } C_n/\text{Total area}] \times 100$$

Where n is the number of carbon atom in the hydrocarbon molecule.

For example;

$$\text{Carbon mole \% of } C_2 = [343.12 / 7305.18] \times 100$$

$$= 4.6969$$

$$\text{Carbon mole \% of } C_3 = [888.76 / 7305.18] \times 100$$

$$= 12.1662$$

The carbon mole% of each product which is obtained from above calculation is shown in Table A3.

Table A5 % Mole of carbon derived by normalization method.

Number of Carbon	% Mole of carbon
C_2	4.6969
C_3	12.1662
C_4	13.6782
C_5	0.3008
C_6	0.7369
C_7	0.0000
C_8	0.3858
B	1.7551
T	12.4843
X	26.9774
C_9	26.8184
Total	100

(Catalyst; 0.7%AgHZ11, Reaction temperature: 425°C, W/F: 10.25 g.hr/mol, Carrier gas: nitrogen, Time on stream: 1 hour)

APPENDIX B

REACTION DATA

Table B1 Product distribution from ethanol conversion over HZ28.

(Reaction temperature: 425°C, W/F: 6.75 g.hr/mol, Carrier gas: nitrogen)

Component	**%Mole of Carbons**						
	Time on stream(hr)						
	0.083	1	2	3	4	5	6
C2	61.49	27.36	28.58	26.67	27.29	27.40	29.22
C3	16.43	20.46	21.20	20.85	20.73	20.97	20.72
C4	2.82	23.82	22.72	23.90	22.88	23.64	22.38
C5	3.29	3.78	3.52	3.67	3.56	3.69	3.57
C6	1.26	3.10	2.38	2.67	2.53	2.64	2.33
Benzene	0.52	0.70	0.69	0.72	0.69	0.72	0.67
C7	0.16	0.59	0.32	0.50	0.43	0.41	0.40
Toluene	1.98	2.85	2.85	2.97	2.90	2.93	2.80
C8	0.00	0.24	0.14	0.24	0.26	0.21	0.16
Ethylbenzene	0.58	0.90	0.89	0.93	0.91	0.92	0.90
m/p-Xylene	3.76	5.13	5.33	5.43	5.46	5.40	5.46
o-Xylene	0.78	1.10	1.25	1.24	1.39	1.15	1.20
C9+	6.92	9.97	10.15	10.20	10.97	9.93	10.19
Total	100	100	100	100	100	100	100

Table B2 Product distribution from ethanol conversion over HZ28.

(Reaction temperature: 425°C, W/F: 10.25 g.hr/mol, Carrier gas: nitrogen)

Component	%Mole of Carbons						
	Time on stream(hr)						
	0.083	1	2	3	4	5	6
C2	24.62	14.77	14.84	14.14	14.45	14.02	14.78
C3	21.16	19.44	19.34	19.46	19.78	19.82	19.44
C4	22.55	23.92	23.29	24.15	24.33	26.01	23.50
C5	2.88	3.18	2.93	3.00	3.09	3.63	3.13
C6	1.66	2.85	2.75	2.91	2.85	3.36	2.80
Benzene	0.74	0.99	0.95	0.99	0.99	0.98	0.98
C7	0.22	0.73	0.40	0.67	0.50	0.85	0.75
Toluene	3.25	4.98	4.90	5.03	5.05	4.79	4.98
C8	0.00	0.24	0.24	0.27	0.26	0.25	0.25
Ethylbenzene	0.87	1.39	1.37	1.40	1.40	1.34	1.42
m/p-Xylene	5.50	8.13	8.33	8.48	8.53	7.94	8.63
o-Xylene	1.41	2.12	2.25	2.22	2.21	2.03	2.27
C9+	15.15	17.27	18.42	17.28	16.55	14.99	17.07
Total	100	100	100	100	100	100	100

Table B3 Product distribution from ethanol conversion over HZ28.

(Reaction temperature: 425°C, W/F: 13.50 g.hr/mol, Carrier gas: nitrogen)

Component	%Mole of Carbons						
	Time on stream (hr)						
	0.083	1	2	3	4	5	6
C2	13.61	9.69	8.83	9.07	9.49	9.00	9.08
C3	16.65	16.81	16.47	16.82	16.89	16.12	16.75
C4	18.74	21.44	22.14	22.15	21.28	20.47	21.77
C5	2.09	2.24	2.34	2.34	2.29	2.21	2.33
C6	1.73	2.52	2.80	2.77	2.59	2.55	2.75
Benzene	0.85	1.12	1.17	1.19	1.17	1.12	1.19
C7	0.10	0.40	0.64	0.63	0.45	0.45	0.58
Toluene	4.46	6.21	6.62	6.47	6.44	6.22	6.56
C8	0.00	0.21	0.30	0.19	0.25	0.22	0.22
Ethylbenzene	1.10	1.59	1.73	1.66	1.65	1.53	1.69
m/p-Xylene	7.25	9.96	10.59	10.33	10.58	9.76	10.61
o-Xylene	2.09	3.20	3.29	3.20	3.38	3.00	3.37
C9+	31.33	24.60	23.07	23.17	23.55	27.36	23.11
Total	100	100	100	100	100	100	100

Table B4 Product distribution from ethanol conversion over HZ28.

(Reaction temperature: 425°C, W/F: 20.25 g.hr/mol, Carrier gas: nitrogen)

	%Mole of Carbons						
	Time on stream (hr)						
Component	0.083	1	2	3	4	5	6
C2	11.33	6.77	6.80	6.55	7.89	7.40	7.09
C3	21.25	18.70	16.95	17.88	18.02	17.90	17.71
C4	25.57	26.84	22.26	24.92	21.31	22.22	22.79
C5	1.42	1.46	1.27	1.23	1.16	1.23	1.25
C6	1.98	3.17	2.38	2.57	1.74	2.17	2.41
Benzene	1.45	1.87	1.69	1.83	1.71	1.77	1.79
C7	0.00	0.67	0.44	0.44	0.18	0.41	0.40
Toluene	7.22	9.24	9.12	9.29	8.55	8.80	8.90
C8	0.20	0.16	0.21	0.36	0.26	0.17	0.23
Ethylbenzene	0.97	1.55	1.56	1.49	1.20	1.28	1.32
m/p-Xylene	9.24	10.89	12.77	11.63	11.33	11.33	11.36
o-Xylene	2.64	3.47	4.13	3.99	3.92	3.71	3.61
C9+	16.73	15.22	20.42	17.82	22.73	21.60	21.15
Total	100	100	100	100	100	100	100

Table B5 Product distribution from ethanol conversion over HZ28.

(Reaction temperature: 425°C, W/F: 27.0 g.hr/mol, Carrier gas: nitrogen)

Component	%Mole of Carbons						
	Time on stream (hr)						
	0.083	1	2	3	4	5	6
Ethylene	8.14	5.47	5.72	5.71	5.82	5.83	5.82
Propylene	17.46	16.00	16.19	16.66	16.62	16.62	16.15
C4	22.05	22.37	22.05	22.31	21.76	21.63	20.66
C5	1.00	1.02	0.98	0.99	0.97	0.98	1.09
C6	1.77	2.13	1.92	2.00	2.03	1.92	1.85
Benzene	1.62	1.99	2.02	2.06	2.06	2.04	2.04
C7	0.00	0.43	0.37	0.36	0.27	0.34	0.35
Toluene	8.41	10.46	10.28	10.29	10.16	10.00	9.87
C8	0.15	0.21	0.25	0.20	0.29	0.13	0.26
Ethylbenzene	1.04	1.47	1.37	1.33	1.28	1.25	1.27
m/p-Xylene	10.60	12.98	12.56	12.56	12.37	12.12	11.91
o-Xylene	3.63	4.31	4.27	4.13	4.02	4.09	4.09
C9+	24.15	21.16	22.01	21.39	22.35	23.05	24.64
Total	100	100	100	100	100	100	100

Table B6 Product distribution from ethanol conversion over HZ11.

(Reaction temperature: 425^{o}C, W/F: 10.25 g.hr/mol, Carrier gas: nitrogen)

Component	%Mole of Carbons						
	Time on stream (hr)						
	0.083	1	2	3	4	5	6
C2	8.38	5.85	5.27	5.21	5.91	6.00	6.60
C3	20.63	19.34	17.65	16.80	18.11	17.92	18.26
C4	24.78	24.30	21.91	20.76	22.01	22.71	22.94
C5	0.78	0.79	0.67	0.69	0.62	0.85	0.77
C6	1.28	1.48	1.48	1.43	1.33	1.55	1.52
Benzene	1.89	2.80	2.67	2.50	2.58	2.42	2.34
C7	0.00	0.00	0.00	0.00	0.00	0.12	0.00
Toluene	7.93	11.39	11.06	10.63	10.86	10.50	10.17
C8	0.00	0.15	0.10	0.13	0.08	0.12	0.07
Ethylbenzene	0.66	0.93	0.97	0.95	1.02	1.13	1.13
m/p-Xylene	7.36	10.15	10.41	10.15	10.86	11.06	10.95
o-Xylene	2.23	3.43	3.37	3.44	3.55	3.46	3.37
C9+	24.08	19.38	24.45	27.32	23.06	22.16	21.89
Total	100	100	100	100	100	100	100

Table B7 Product distribution from ethanol conversion over 0.7%AgHZ11.

(Reaction temperature: 425°C, W/F: 10.25 g.hr/mol, Carrier gas: nitrogen)

Component	**%Mole of Carbons**						
	Time on stream (hr)						
	0.083	1	2	3	4	5	6
C2	8.42	4.70	4.29	4.42	4.68	4.72	5.14
C3	12.12	12.17	12.81	13.25	13.28	13.47	14.08
C4	13.67	13.68	14.77	15.53	15.21	16.00	16.84
C5	0.51	0.30	0.29	0.36	0.40	0.44	0.49
C6	0.82	0.74	0.76	0.81	0.79	0.89	0.96
Benzene	1.47	1.76	1.90	1.93	1.88	1.90	1.85
C7	0.00	0.00	0.00	0.00	0.00	0.00	0.00
Toluene	11.47	12.48	12.26	12.19	11.64	11.43	10.95
C8	0.35	0.39	1.00	0.63	0.60	0.82	0.34
Ethylbenzene	0.53	0.57	0.62	0.64	0.61	0.69	0.70
m/p-Xylene	18.19	19.57	19.30	18.16	17.43	17.97	17.17
o-Xylene	6.05	6.84	6.81	6.68	6.09	6.39	5.93
C9+	26.41	26.82	25.18	25.39	27.40	25.28	25.54
Total	100	100	100	100	100	100	100

Table B8 Product distribution from ethanol conversion over reg-0.7%AgHZ11.

(Reaction temperature: 425°C, W/F: 10.25 g.hr/mol, Carrier gas: nitrogen)

Component	**%Mole of Carbons**						
	Time on stream (hr)						
	0.083	1	2	3	4	5	6
C2	6.86	5.26	5.23	5.25	5.97	6.52	7.33
C3	19.00	16.50	15.52	14.98	15.05	16.47	16.40
C4	22.67	20.94	19.99	20.08	19.14	22.03	21.31
C5	0.48	0.47	0.51	0.57	0.60	0.79	0.81
C6	1.09	1.09	1.11	1.19	1.11	1.42	1.37
Benzene	2.41	2.23	2.08	1.87	1.80	1.79	1.57
C7	0.00	0.00	0.00	0.06	0.00	0.07	0.15
Toluene	12.93	12.27	11.39	10.36	10.27	9.85	9.00
C8	0.00	0.00	0.16	0.12	0.10	0.08	0.00
Ethylbenzene	0.53	0.69	0.84	0.82	0.83	0.92	0.86
m/p-Xylene	15.57	16.16	16.30	15.10	15.94	14.72	14.32
o-Xylene	4.67	5.23	5.44	4.97	5.08	4.49	4.37
C9+	13.79	19.18	21.44	24.62	24.11	20.84	22.51
Total	100	100	100	100	100	100	100

Table B9 Product distribution from ethanol conversion over 1.3%AgHZ11.

(Reaction temperature: 425°C, W/F: 10.25 g.hr/mol, Carrier gas: nitrogen)

Component	**%Mole of Carbons**						
	Time on stream (hr)						
	0.083	1	2	3	4	5	6
C2	14.47	5.40	4.91	4.79	5.59	5.93	6.57
C3	12.21	12.02	10.79	11.74	13.52	14.71	14.73
C4	13.92	15.30	13.43	15.25	17.07	19.22	18.66
C5	0.99	0.50	0.46	0.51	0.57	0.69	0.77
C6	0.90	0.96	0.86	0.98	1.11	1.38	1.39
Benzene	1.19	1.46	1.40	1.33	1.53	1.54	1.49
C7	0.00	0.00	0.00	0.00	0.00	0.00	0.00
Toluene	10.58	12.06	11.29	9.59	10.43	9.63	8.93
C8	0.34	0.73	0.67	0.78	0.77	0.34	0.26
Ethylbenzene	0.65	0.66	0.71	0.65	0.79	0.88	0.89
m/p-Xylene	12.43	19.63	20.19	16.72	18.40	16.48	15.16
o-Xylene	4.44	6.72	7.32	5.73	6.11	5.36	4.85
C9+	27.87	24.56	27.96	31.92	24.10	23.83	26.30
Total	100	100	100	100	100	100	100

Table B10 Product distribution from ethanol conversion over reg-1.3%AgHZ11.

(Reaction temperature: 425°C, W/F: 10.25 g.hr/mol, Carrier gas: nitrogen)

Component	**%Mole of Carbons**						
	Time on stream (hr)						
	0.083	1	2	3	4	5	6
C2	5.24	4.85	4.94	5.37	5.75	6.52	7.16
C3	11.80	12.07	12.56	13.00	13.78	14.34	15.01
C4	13.36	14.14	15.27	15.94	17.62	17.96	18.71
C5	0.33	0.38	0.45	0.60	0.72	0.81	0.93
C6	0.61	0.76	0.87	1.02	1.26	1.24	1.33
Benzene	1.84	1.73	1.72	1.68	1.64	1.61	1.62
C7	0.00	0.00	0.00	0.00	0.06	0.06	0.07
Toluene	13.80	12.83	11.83	11.16	10.23	9.83	9.57
C8	0.09	0.53	0.74	0.54	0.83	0.68	0.81
Ethylbenzene	0.55	0.61	0.70	0.71	0.82	0.85	0.95
m/p-Xylene	20.19	19.62	18.42	17.19	16.24	15.59	15.38
o-Xylene	6.99	6.89	6.45	6.06	5.45	5.50	4.95
C9+	25.20	25.58	26.05	26.72	25.60	25.00	23.50
Total	100	100	100	100	100	100	100

Table B11 Product distribution from ethanol conversion over 3.0%AgHZ11.

(Reaction temperature: 425°C, W/F: 10.25 g.hr/mol, Carrier gas: nitrogen)

Component	%Mole of Carbons						
	Time on stream (hr)						
	0.083	1	2	3	4	5	6
C2	29.87	7.33	6.24	6.40	6.63	7.50	8.30
C3	4.15	8.72	8.63	9.33	9.83	11.33	12.89
C4	8.50	12.36	12.19	12.70	12.77	14.88	17.21
C5	0.94	0.64	0.59	0.70	0.75	0.98	1.12
C6	0.74	0.98	0.97	0.97	1.04	1.14	1.62
Benzene	1.14	1.06	0.96	0.97	1.03	0.99	0.96
C7	0.00	0.00	0.00	0.00	0.00	0.00	0.26
Toluene	8.89	12.18	10.20	9.54	9.76	8.86	7.93
C8	0.21	0.55	0.46	0.10	0.07	0.15	0.20
Ethylbenzene	1.17	1.04	0.79	0.75	0.88	0.84	0.87
m/p-Xylene	10.08	18.21	16.26	15.47	18.22	16.78	15.42
o-Xylene	3.23	6.06	5.49	5.33	6.02	5.43	4.73
C9+	31.09	30.88	37.22	37.73	33.00	31.13	28.50
Total	100	100	100	100	100	100	100

Table B12 Product distribution from ethanol conversion over reg-3.0%AgHZ11.

(Reaction temperature: 425°C, W/F: 10.25 g.hr/mol, Carrier gas: nitrogen)

Component	**%Mole of Carbons**						
	Time on stream (hr)						
	0.083	1	2	3	4	5	6
C2	8.72	6.11	5.96	6.08	6.41	6.85	7.48
C3	8.89	8.13	9.15	9.67	11.23	12.38	13.32
C4	10.54	10.66	12.10	12.04	14.15	15.37	16.54
C5	0.45	0.45	0.52	0.51	0.61	0.71	0.84
C6	0.59	0.70	0.82	0.82	1.04	1.15	1.28
Benzene	1.78	1.24	1.27	1.25	1.29	1.31	1.31
C7	0.00	0.00	0.00	0.00	0.00	0.00	0.00
Toluene	13.86	11.80	12.08	11.51	11.21	10.62	10.26
C8	0.17	0.70	0.60	0.56	0.43	0.71	0.62
Ethylbenzene	0.92	0.73	0.77	0.73	0.80	0.84	1.01
m/p-Xylene	14.91	15.49	17.79	17.91	18.51	18.30	18.57
o-Xylene	5.47	5.20	6.05	6.14	6.17	6.06	5.87
C9+	33.70	38.78	32.89	32.78	28.16	25.70	22.90
Total	100	100	100	100	100	100	100

Table B13 Product distribution from ethanol conversion over 4.8%AgHZ11.

(Reaction temperature: 425°C, W/F: 10.25 g.hr/mol, Carrier gas: nitrogen)

Component	**%Mole of Carbons**						
	Time on stream (hr)						
	0.083	1	2	3	4	5	6
C2	61.44	15.38	13.19	13.06	14.68	16.54	17.94
C3	0.00	10.25	11.19	13.73	16.87	18.51	19.54
C4	3.54	11.54	11.79	14.35	18.04	19.23	21.06
C5	0.33	1.28	1.17	1.36	1.84	2.13	1.98
C6	0.00	0.77	0.81	0.89	1.42	1.44	1.59
Benzene	1.61	1.19	1.15	1.11	1.15	1.09	1.03
C7	0.00	0.00	0.00	0.00	0.11	0.13	0.15
Toluene	4.66	8.58	7.80	7.10	6.84	6.02	5.26
C8	0.00	0.16	0.08	0.10	0.30	0.32	0.21
Ethylbenzene	1.63	1.16	0.91	0.85	1.02	1.05	1.16
m/p-Xylene	3.04	10.99	10.69	11.15	11.84	10.88	10.17
o-Xylene	0.89	3.49	3.57	3.60	3.49	2.97	2.79
C9+	22.85	35.23	37.65	32.71	22.40	19.69	17.12
Total	100	100	100	100	100	100	100

Table B14 Product distribution from ethanol conversion over reg-4.8%AgHZ11.

(Reaction temperature: 425°C, W/F: 10.25 g.hr/mol, Carrier gas: nitrogen)

	%Mole of Carbons						
	Time on stream (hr)						
Component	0.083	1	2	3	4	5	6
C2	30.34	11.56	12.30	12.69	12.69	15.87	15.64
C3	8.39	10.63	11.37	12.82	14.16	14.84	16.46
C4	8.69	13.01	14.07	16.07	17.83	16.88	20.49
C5	1.07	1.27	1.43	1.67	1.89	1.82	2.42
C6	0.30	0.88	1.05	1.35	1.59	1.10	1.84
Benzene	1.58	1.06	1.01	0.98	0.99	0.90	0.90
C7	0.00	0.00	0.07	0.11	0.11	0.12	0.23
Toluene	7.85	10.53	8.57	7.65	7.26	6.22	5.54
C8	0.17	0.51	0.83	0.26	0.27	0.21	0.47
Ethylbenzene	2.04	1.33	1.22	1.22	1.27	1.17	1.26
m/p-Xylene	8.15	16.86	16.05	15.03	14.82	13.39	11.96
o-Xylene	2.71	5.21	4.69	4.35	4.09	3.59	3.13
C9+	28.70	27.15	27.34	25.80	23.03	23.88	19.66
Total	100	100	100	100	100	100	100

Table B15 Product distribution from ethanol conversion over 3.0%AgHZ28.

(Reaction temperature: 425°C, W/F: 10.25 g.hr/mol, Carrier gas: nitrogen)

Component	%Mole of Carbons						
	Time on stream (hr)						
	0.083	1	2	3	4	5	6
C2	93.56	88.06	90.94	91.89	91.89	92.75	93.52
C3	0.00	0.00	0.00	0.00	0.00	0.00	0.00
C4	1.80	2.46	2.43	2.37	2.37	2.33	2.33
C5	0.00	0.22	0.20	0.18	0.18	0.16	0.16
C6	0.00	0.00	0.00	0.00	0.00	0.00	0.00
Benzene	0.47	0.26	0.21	0.20	0.20	0.19	0.18
C7	0.00	0.00	0.00	0.00	0.00	0.00	0.00
Toluene	1.20	0.68	0.52	0.48	0.48	0.42	0.39
C8	0.00	0.00	0.00	0.00	0.00	0.00	0.00
Ethylbenzene	0.33	0.25	0.21	0.19	0.19	0.17	0.16
m/p-Xylene	0.69	0.84	0.79	0.69	0.69	0.66	0.59
o-Xylene	0.20	0.23	0.21	0.18	0.18	0.17	0.16
C9+	1.73	7.01	4.50	3.83	3.83	3.14	2.51
Total	100	100	100	100	100	100	100

Table B16 Product distribution from ethanol conversion over 3.0%AgHZ28.

(Reaction temperature: 425°C, W/F: 10.25 g.hr/mol, Carrier gas: 26%hydrogen/nitrogen)

Component	%Mole of Carbons						
	Time on stream (hr)						
	0.083	1	2	3	4	5	6
C2	83.54	19.92	19.04	21.27	20.04	18.87	18.32
C3	5.67	18.97	18.40	19.49	19.32	18.55	18.61
C4	5.24	27.06	26.20	24.88	25.80	25.89	26.52
C5	0.50	2.92	3.72	3.33	3.62	3.70	3.80
C6	0.00	2.71	2.80	2.01	2.85	3.06	3.08
Benzene	0.21	0.73	0.74	0.72	0.76	0.77	0.78
C7	0.00	0.20	0.37	0.15	0.18	0.39	0.37
Toluene	1.19	3.60	3.66	3.49	3.70	3.56	3.82
C8	0.00	0.26	0.31	0.11	0.26	0.34	0.30
Ethylbenzene	0.29	1.04	1.08	1.02	1.06	1.07	1.12
m/p-Xylene	1.03	5.95	6.39	6.31	6.35	6.57	6.67
o-Xylene	0.32	1.31	1.51	1.35	1.37	1.52	1.61
C9+	2.00	15.34	15.78	15.86	14.69	15.71	15.00
Total	100	100	100	100	100	100	100

APPENDIX C

SURFACE AREA

Table C1 Data from gas adsorption analysis of HZ11

P/P_0	Volume (cc/g)	BET
5.04E-02	168.7308	2.52E-01
7.59E-02	174.0475	3.78E-01
1.01E-01	178.7733	5.04E-01
1.25E-01	185.0325	6.19E-01
1.51E-01	189.2667	7.54E-01
1.77E-01	192.5125	8.92E-01
2.02E-01	195.7183	1.04E-01
2.27E-01	201.6050	1.16E-01
2.52E-01	204.1383	1.32E+00
2.77E-01	205.4700	1.50E+00
3.01E-01	213.9775	1.62E+00

Surface area = 643.9 m^2/g

Table C2 Data from gas adsorption analysis of 0.7%AgHZ11

P/P_0	**Volume (cc/g)**	**BET**
5.25E-02	157.4082	2.81E-01
7.51E-02	163.5568	3.97E-01
1.01E-01	168.9336	5.30E-01
1.26E-01	173.6712	6.64E-01
1.51E-01	177.5356	8.03E-01
1.77E-01	184.4712	9.32E-01
2.01E-01	188.1616	1.07E+00
2.27E-01	191.2212	1.23E+00
2.51E-01	197.0493	1.36E+00
2.77E-01	200.4541	1.53E+00
3.02E-01	203.2466	1.70E+00

Surface area = 622.93 m^2/g

Table C3 Data from gas adsorption analysis of 1.3%AgHZ11

P/P_0	Volume (cc/g)	BET
4.98E-02	145.3153	2.89E-01
7.56E-02	150.2197	4.36E-01
1.00E-01	155.7752	5.74E-01
1.26E-01	159.9642	7.19E-01
1.52E-01	163.6299	8.73E-01
1.76E-01	168.8679	1.01E+00
2.00E-01	172.3328	1.16E+00
2.27E-01	175.3387	1.34E-01
2.51E-01	180.6474	1.48E+00
2.76E-01	183.6263	1.66E+00
3.01E-01	185.9117	1.85E+00

Surface area = 570.2 m^2/g

Table C4 Data from gas adsorption analysis of 3.0%AgHZ11

P/P_0	Volume (cc/g)	BET
4.95E-02	122.4553	3.41E-01
7.62E-02	126.0760	5.24E-01
1.01E-01	129.8548	6.89E-01
1.26E-01	132.6475	8.74E-01
1.50E-01	136.6207	1.04E+00
1.77E-01	139.3352	1.23E+00
2.00E-01	143.4045	1.40E+00
2.27E-01	145.9207	1.61E+00
2.49E-01	150.9247	1.76E+00
2.77E-01	153.3927	2.00E+00
2.99E-01	158.6626	2.15E+00

Surface area = 481.0 m^2/g

Table C5 Data from gas adsorption analysis of 4.8%AgHZ11

P/P_0	Volume (cc/g)	BET
5.11E-02	94.5318	4.63E-01
7.61E-02	97.5824	6.75E-01
1.01E-01	100.1082	9.01E-01
1.27E-01	102.7353	1.13E+00
1.52E-01	104.6665	1.37E+00
1.77E-01	105.7924	1.63E+00
2.03E-01	106.7041	1.91E+00
2.58E-01	110.6647	2.11E+00
2.51E-01	112.7423	2.38E+00
2.77E-01	114.2718	2.68E+00
3.00E-01	119.0953	2.88E+00

Surface area = 356.6 m^2/g

Table C6 Data from gas adsorption analysis of HZ28

P/P_0	Volume (cc/g)	BET
5.04E-02	146.7693	2.89E-01
7.56E-02	151.7979	4.31E-01
1.00E-01	157.0493	5.68E-01
1.26E-01	161.2628	7.14E-01
1.52E-01	164.3557	8.70E-01
1.77E-01	167.6614	1.03E+00
2.02E-01	171.0879	1.18E+00
2.67E-01	173.3179	1.35E+00
2.52E-01	175.2936	1.54E+00
2.76E-01	182.0150	1.67E+00
3.01E-01	185.2021	1.86E+00

Surface area = 560.31 m^2/g

Table C7 Data from gas adsorption analysis of 3.0%AgHZ28

P/P_0	**Volume (cc/g)**	**BET**
5.12E-02	129.2869	3.43E-01
7.63E-02	133.7730	4.94E-01
1.02E-01	136.9854	6.62E-01
1.26E-01	141.1949	8.17E-01
1.52E-01	144.2847	9.92E-01
1.77E-01	147.0825	1.17E+00
2.01E-01	151.7409	1.33E+00
2.28E-01	153.7080	1.53E+00
2.53E-01	155.1876	1.74E+00
2.76E-01	160.5299	1.90E+00
3.03E-01	162.4175	2.14E+00

Surface area = 493.8 m^2/g

AUTHOR BIOGRAPHY

Miss Suratsawadee Suwannaran was born on August 3, 1978 in Chantaburi. She received a Bachelor degree of Applied Science in Industrial Chemistry from King Mongkut's Institute of North Bangkok in 2000. She has been graduated student of the Program of Petrochemicals and Hydrocarbon Chemistry, Graduate School, King Mongkut's Institute of Technology Ladkrabang, since 2001.